

# Bayesian Safe Policy Learning with Chance Constrained Optimization: Application to Military Security Assessment during the Vietnam War\*

Zeyang Jia<sup>†</sup>Eli Ben-Michael<sup>‡</sup>Kosuke Imai<sup>§</sup>

July 19, 2023

## Abstract

Algorithmic and data-driven decisions and recommendations are commonly used in high-stakes decision-making settings such as criminal justice, medicine, and public policy. We investigate whether it would have been possible to improve a security assessment algorithm employed during the Vietnam War, using outcomes measured immediately after its introduction in late 1969. This empirical application raises several methodological challenges that frequently arise in high-stakes algorithmic decision-making. First, before implementing a new algorithm, it is essential to characterize and control the risk of yielding worse outcomes than the existing algorithm. Second, the existing algorithm is deterministic, and learning a new algorithm requires transparent extrapolation. Third, the existing algorithm involves discrete decision tables that are common but difficult to optimize over.

To address these challenges, we introduce the Average Conditional Risk (ACRisk), which first quantifies the risk that a new algorithmic policy leads to worse outcomes for subgroups of individual units and then averages this over the distribution of subgroups. We also propose a Bayesian policy learning framework that maximizes the posterior expected value while controlling the posterior expected ACRisk. This framework separates the estimation of heterogeneous treatment effects from policy optimization, enabling flexible estimation of effects and optimization over complex policy classes. We characterize the resulting chance-constrained optimization problem as a constrained linear programming problem. Our analysis shows that compared to the actual algorithm used during the Vietnam War, the learned algorithm assesses most regions as more secure and emphasizes economic and political factors over military factors.

**Keywords:** algorithmic decisions, Bayesian nonparametrics, conditional average treatment effect, decision tables, risk

---

\*We acknowledge the partial support from Cisco Systems, Inc. (CG# 2370386), National Science Foundation (SES-2051196), and Sloan Foundation (Economics Program; 2020-13946).

<sup>†</sup>Ph.D. Student, Department of Statistics, Harvard University. 1 Oxford Street, Cambridge MA 02138. Email: [zeyangjia@fas.harvard.edu](mailto:zeyangjia@fas.harvard.edu)

<sup>‡</sup>Assistant Professor, Department of Statistics & Data Science and Heinz College of Information Systems & Public Policy, Carnegie Mellon University. 4800 Forbes Avenue, Hamburg Hall, Pittsburgh PA 15213. Email: [ebenmichael@cmu.edu](mailto:ebenmichael@cmu.edu) URL: [ebenmichael.github.io](https://ebenmichael.github.io)

<sup>§</sup>Professor, Department of Government and Department of Statistics, Harvard University. 1737 Cambridge Street, Institute for Quantitative Social Science, Cambridge MA 02138. Email: [imai@harvard.edu](mailto:imai@harvard.edu) URL: <https://imai.fas.harvard.edu>

# 1 Introduction

Algorithmic and data-driven decisions and recommendations have long been used in areas as diverse as credit markets (Lauer, 2017) and war (Daddis, 2012). They are now increasingly integral to many aspects of today’s society, including online advertising (e.g., Li et al., 2010; Tang et al., 2013; Schwartz et al., 2017), medicine (e.g., Kamath et al., 2001; Nahum-Shani et al., 2018), and criminal justice (e.g., Imai et al., 2023; Greiner et al., 2020). A primary challenge when applying data-driven policies to consequential decision tasks is to characterize and control the risk associated with any new policies learned from the data. Stakeholders in fields such as medicine, public policy, and the military may be concerned that the adoption of new data-derived policies could inadvertently lead to worse outcomes for some individuals in certain settings.

In this paper, we consider a particularly high-stakes setting, analyzing a United States military security assessment policy that saw active use in the Vietnam War. During the war, the United States military developed a data-driven scoring system called the Hamlet Evaluation System (HES) to produce a security score for each region (PACAF, 1969); commanders used these scores to make air strike decisions. A recent analysis based on a regression discontinuity design shows that the airstrikes had significantly negative effects on development outcomes including regional safety, economic, and civic society measures, and so were broadly counter-productive (Dell and Querubin, 2018). We consider whether it would have been possible to improve the HES to reflect this fact, using contemporaneous data collected by the US military and related agencies, while avoiding the risk of worsening development outcomes in many regions by changing the evaluation system.

In particular, the original HES was composed of various “sub-model scores” that measured different aspects of each region (e.g., economic variables, local administration, enemy military presence) based on survey responses. It then combined these into a single security score through a three-level hierarchical aggregation using pre-defined decision tables that determined how to consolidate different scores. The security scores were then presented to Air Force commanders, who used them to make targeting decisions. Our goal, then, is to modify the HES by changing the underlying decision tables, finding those tables that optimize various development objectives, while limiting the risk of deteriorating these objectives in individual regions.

This empirical question poses several methodological challenges that are commonly encountered in high-stakes data-driven decision making settings. First, we want to characterize and control the risk that a new learned decision, classification, or recommendation policy may lead to worse outcomes for some groups of regions (i.e. individual units). Second, the HES is a deterministic function of the input data, implying that extrapolation is necessary to learn new policies. Third, the security score is produced via a series of aggregations using decision tables. Indeed, decision tables are widely used in many public policy and medical decision making settings (e.g., risk scores in the US criminal justice system Greiner et al., 2020; Imai et al., 2023) but are challenging to optimize over in practice.

To address these challenges, we introduce a risk measure, the Average Conditional Risk (ACRisk), that first quantifies the risk of a given policy for groups of individual units with a specified set of covariates and then averages this conditional risk over the distribution of the covariates. In contrast to

existing risk measures that characterize the uncertainty around the average performance of the policy (e.g., [Delage and Mannor, 2010](#); [Vakili and Zhao, 2015](#); [Bai et al., 2022](#)), the ACRisk measures the extent to which a learned policy negatively affects subgroups. This allows us to better characterize the potential heterogeneous risks of applying a new policy.

With this risk measure in hand, we propose a Bayesian safe policy learning framework that maximizes the posterior expected value given the observed data while controlling the posterior expected ACRisk. We formulate this as a chance-constrained optimization problem and show how to efficiently solve it using samples from the posterior distribution of the conditional average treatment effect (CATE).

The primary advantage of the proposed framework is its flexibility. Because the chance-constrained optimization problem only relies on posterior samples, one can use popular Bayesian nonparametric regression models such as BART and Gaussian Process regression ([Rasmussen and Williams, 2006](#); [Chipman et al., 2010](#); [Branson et al., 2019](#)), while efficiently finding an optimal policy within a complex policy class. This is especially helpful in settings such as ours with limited or no covariate overlap, where our framework allows for flexible extrapolation through the Bayesian prior. In contrast, frequentist notions of safe policy learning rely on robust optimization and require solving a minimax optimization problem over both the class of potential models and the class of potential policies, making it difficult to consider nonparametric models and complex policy classes at the same time ([Pu and Zhang, 2020](#); [Kallus and Zhou, 2021](#); [Ben-Michael et al., 2022](#); [Zhang et al., 2022](#)).

We show through simulation studies that controlling the posterior expected ACRisk effectively limits the ACRisk across various scenarios, reducing the risk of harming certain subgroups of units. We also find that although the proposed methodology is designed to be conservative, under some settings with a low signal-to-noise ratio, it yields a new policy whose average value is higher than a policy learned without the safety constraint. This is evidence that the proposed safety constraint can effectively regularize the policy optimization problem.

In our empirical analysis, we apply the proposed methodology to find adaptations to the HES that lead to better outcomes overall — as measured by military, economic, and social objectives — while limiting the posterior probability that some regions experience worse outcomes under the new system than under the original HES. We consider two policy learning problems — one where we only change the decision table used in the last layer of the hierarchical aggregation, and another where we modify the decision tables used in all of the three-level hierarchical aggregation at the same time. To deal with the latter complex case, we develop a stochastic optimization algorithm, based on random walks on partitions of directed acyclic graphs, that is generally applicable to decision tables. Our analysis consistently shows that the original HES is too pessimistic—assessing regions as too insecure—and places too much emphasis on military factors, while data-derived adaptations to the HES assess regions as more secure and rely more on economic and social factors to produce regional security scores.

**Related literature.** Recent years have witnessed a growing interest among statisticians and machine learning researchers in finding optimal policies from randomized experiments and observational studies (e.g. [Beygelzimer and Langford, 2009](#); [Qian and Murphy, 2011](#); [Dudík et al., 2011](#); [Zhao et al., 2012](#);

Zhang et al., 2012; Swaminathan and Joachims, 2015; Luedtke and Van Der Laan, 2016; Zhou et al., 2017; Kitagawa and Tetenov, 2018; Kallus, 2018; Athey and Wager, 2021; Zhou et al., 2022). These works typically consider the following two steps under a frequentist framework — first characterize the average performance, or value, of a given policy via the CATE, and then learn an optimal policy by maximizing the estimated value based on the observed data.

In contrast, we adopt a Bayesian perspective — first obtain the posterior distribution of the CATE given the observed data, and then learn an optimal policy by maximizing the posterior expected value. Bayesian methods have been widely used for causal inference (see Li et al., 2022b, for a recent review). In particular, BART and Gaussian processes are often used to flexibly estimate the CATE (Hill, 2011; Branson et al., 2019; Taddy et al., 2016; Hahn et al., 2020). However, it appears that the Bayesian approach has been rarely applied to policy learning. Our proposed framework takes advantage of these popular Bayesian nonparametric methods for safe policy learning.

There is also a growing literature on policy learning in scenarios where the CATE is unidentifiable. These include observational studies with unmeasured confounders (Kallus and Zhou, 2021), studies with noncompliance or an instrumental variable (Pu and Zhang, 2020), studies that lack overlap due to deterministic treatment rules (Ben-Michael et al., 2021; Zhang et al., 2022), and utility functions that involve the joint set of potential outcomes (Ben-Michael et al., 2022). These works first partially identify the value of a given policy then find the policy that maximizes the worst-case value using robust optimization. Our approach differs in that we decouple estimation and policy optimization by only relying on posterior samples for policy learning.

In the Reinforcement Learning (RL) literature, various notions of safety have been studied under different names (e.g., safe reinforcement learning, risk averse reinforcement learning, pessimistic reinforcement learning; see Garcia and Fernández (2015)). For example, Geibel and Wyszotzki (2005) control the risk of the agent visiting a “dangerous state” by explicitly imposing a risk constraint when finding an optimal policy. In contrast, Sato et al. (2001) and Vakili and Zhao (2015) use the variance of the return as a penalty term in the objective when finding an optimal policy with a high expected return and low variance. While this RL literature focuses on online settings where the algorithm is designed to avoid risks during exploration, we study the risk of applying data-driven policies in offline settings.

We also extend existing work by developing the notion of ACRisk and using it as a constraint in optimizing the posterior expected value of a new policy. A related literature is *pessimistic offline RL*, which quantifies the risk of a given policy using the lower confidence bound (LCB) of the value, and finds a policy that has the best LCB (Jin et al., 2021; Buckman et al., 2020; Zanette et al., 2021; Xie et al., 2021; Chen and Jiang, 2022; Rashidinejad et al., 2021; Yin and Wang, 2021; Shi et al., 2022; Yan et al., 2022; Uehara and Sun, 2021; Bai et al., 2022; Jin et al., 2022). In contrast, the proposed ACRisk measures the extent to which a new policy negatively affects some groups of individuals when compared to the baseline policy.

Finally, our work is also related to chance constrained optimization, which is widely used in the analysis of decision making under uncertainty (e.g., Schwarm and Nikolaou, 1999; Filar et al., 1995; Delage and Mannor, 2007, 2010; Farina et al., 2016). For example, Delage and Mannor (2010) consider

chance constrained control for Markov Decision Processes. They assume a Gaussian model for the reward distribution and use chance constrained optimization to find a policy that achieves low regret with high posterior probability. Our method considers a more general setup beyond the Gaussian model and uses the posterior expected value of the ACRisk as a constraint, which differs from the existing work.

**Outline of the paper.** The remainder of this paper is organized as follows. Section 2 describes U.S. military security assessment in the Vietnam War, the HES, and the related empirical policy learning problem. Section 3 introduces a formal setup, and Section 4 describes the Bayesian safe policy learning framework and the chance-constrained optimization procedure, as well as implementation via Gaussian Processes and Bayesian Causal Forests. Section 5 presents numerical experiments evaluating our proposal. Section 6 applies the Bayesian safe policy learning method to the Military security assessment problem. Section 7 concludes and discusses limitations and future directions.

## 2 Military Security Assessment during the Vietnam War

During the Vietnam War, the United States Air Force (USAF) conducted numerous air strike campaigns. One factor guiding USAF commanders in making targeting decisions during these missions was a data-driven scoring system called the Hamlet Evaluation System (HES) whose goal was to provide a metric for regional security based on survey data (PACAF, 1969). We briefly describe the HES and its aggregation rules, as well as the policy learning problem we consider. Specifically, we focus on the second version of the HES, which was developed in 1969 and was originally analyzed by Dell and Querubin (2018).

### 2.1 The Hamlet Evaluation System

The HES was based on a total of 169 military, political, and socioeconomic indicators collected quarterly by Civil Operations and Revolutionary Development Support (CORDS), a joint civilian-military agency. These indicators were then categorized and summarized as 20 continuous “sub-model” scores.<sup>1</sup> Each sub-model score ranges from 1 to 5 and measures a different aspect of a given region, such as *Enemy Military Activity*, *Economic Activity*, and *Public Health*. The HES aggregates these 20 continuous-valued sub-model scores into a single integer-valued security score ranging between 1 and 5. After calculating the security score for each region at the beginning of a quarter, USAF commanders used these scores to make air strike decisions during that quarter.

Although several other factors contributed to the determination of eventual air strike targets, Dell and Querubin (2018) show that regions which fell just above a security score threshold — and hence had a higher security score — were less likely to be subject to air strikes than those regions just below the threshold. Using a regression discontinuity design, the authors find that the air strike campaign was largely counter-productive, increasing insurgency activities and decreasing civic engagements.

Given this finding, we investigate whether it is possible to improve the original HES security evaluation with the contemporaneous data available during the war to achieve better outcomes. Specifically,

---

<sup>1</sup>The HES actually produces 19 different sub-model scores from the 169 indicators, but one sub-model score is used twice in the later aggregation. For simplicity and clarity, consider these to be 20 scores.

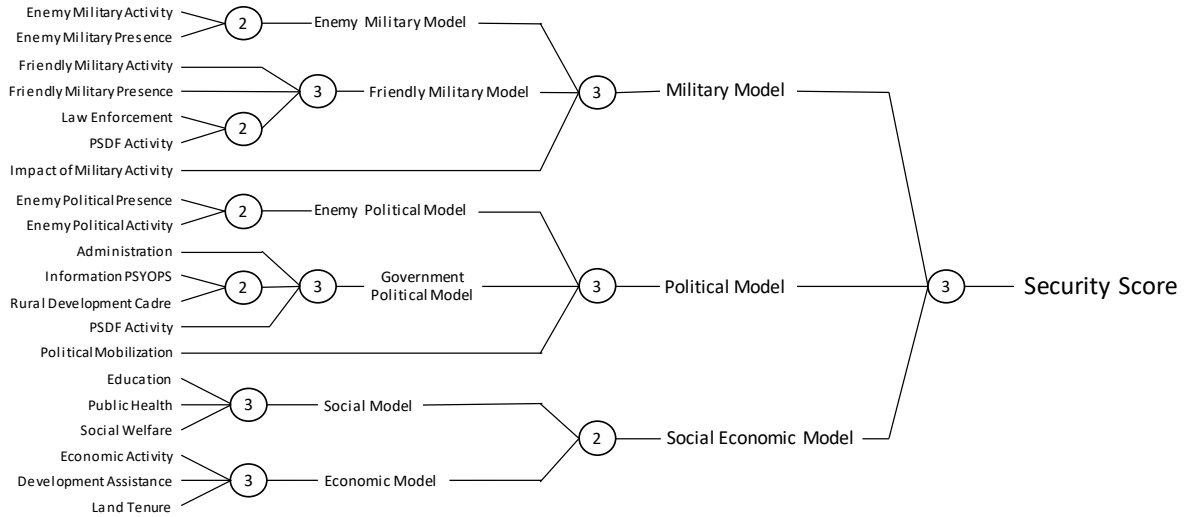


Figure 1: Aggregation of 20 sub-model scores. The Hamlet Evaluation System (HES) uses 20 sub-model scores as inputs, and aggregates them using two-way and three-way decision tables. Each circle corresponds to one aggregation based on the two-way or three-way decision table, and the decision tables used in different circles are the same.

we focus on the first quarter that the HES was deployed (Q4 1969) and use the military impact assessments taken at the beginning of the succeeding quarter (January 1970) as the outcome to measure the efficacy of the HES.

## 2.2 Aggregation via Decision Tables

The HES aggregates 20 continuous sub-model scores to a single integer-valued security score that take a value in  $\{1, 2, 3, 4, 5\}$ , as shown in Figure 1. This hierarchical aggregation process starts by rounding the 20 continuous sub-model scores to the nearest integer in  $\{1, 2, 3, 4, 5\}$ . The security score then is produced through the following three steps. First, 18 out of these 20 rounded sub-model scores are aggregated to six integer-valued model scores relating to military, friendly military, enemy political, government political, social, and economic model scores. Second, the resulting six model scores, along with two remaining inputs (impact of military activity and political mobilization), are aggregated to three higher tier integer-valued scores — Military, Political, and Social Economic model scores. Finally, these three scores are further aggregated to the integer-valued single security score.

At each step of aggregation, the HES uses the two-way or three-way decision table indicated by the number shown in each circle of Figure 1. These tables take two or three integer-valued scores, ranging from 1 to 5, and return a new score, which takes a value in  $\{1, 2, 3, 4, 5\}$ . Figure 2 shows the two-way table, which, for example, maps an input of (2, 3) to an output of 2. The three-way table is shown in Figure S1 of the appendix. In the HES, the same two-way and three-way tables are used across all levels of aggregation.

Since the hierarchical structure of the HES aggregation process contains substantial domain knowledge, we do not attempt to modify the overall aggregation structure of the HES shown in Figure 1. Instead, we focus on improving the two-way and three-way decision tables used in each single aggre-

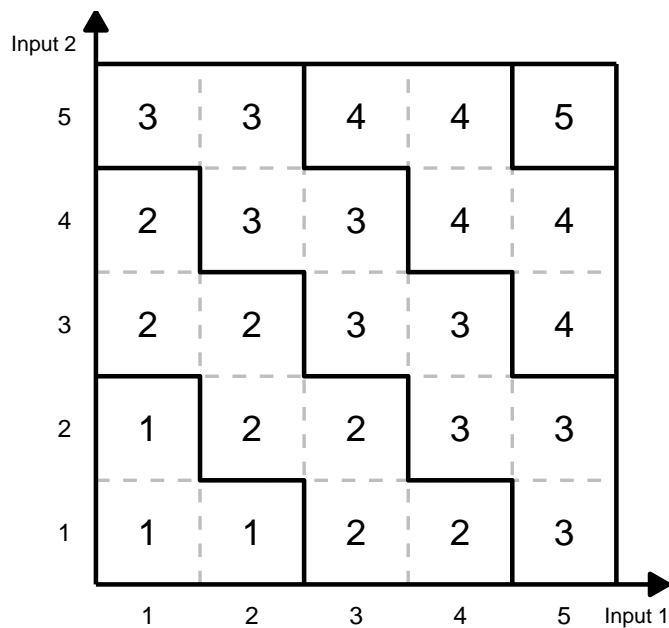


Figure 2: The two-way table used in the Hamlet Evaluation System for aggregating two input scores. The  $(i, j)$  element in the table above shows the output score when the first input is  $i$  and the second input is  $j$ .

gation.

### 2.3 Evidence-based Policy Learning

To measure the impact of air strikes and conduct policy learning, we analyze three binary outcomes that reflect regional security, economy, and civic society. These outcomes are based on survey responses from multiple sources collected in January 1970, after the period of air strikes in the final quarter of 1969 (Dell and Querubin, 2018). During this period, USAF commanders targeted 1024 of the 1954 regions defined by the HES.<sup>2</sup> Our objective is to develop a new decision rule that generates appropriate security scores based on the 20 continuous sub-model scores. It is worth noting that our decision variable is the output security score from the HES rather than the air strike decision itself; air strike decisions are made by commanders. We aim to optimize the way to produce the final security score from the 20 sub-model scores to achieve the best overall outcomes in regional security, economy, and civic society (marginalizing over commanders' airstrike decisions).

This application yields several methodological challenges. First, the stakes of this decision are high and there is potential heterogeneity across regions. This motivates a safe policy learning approach that limits the possibility of generating worse outcome under a new, learned policy for some regions than the under existing policy. Second, the existing policy is a deterministic, rather than stochastic, policy. This means that we must extrapolate in order to estimate the potential outcome under a new policy, due

<sup>2</sup>See Appendix Table S1 and Figure S2 for other summary statistics as well as the average values of the security score and various sub-model scores



to the lack of overlap. Lastly, the existing policy is based on multiple decision tables. Thus, to keep the existing structure of the policy, we must solve a complex optimization problem. We now develop a new Bayesian safe policy framework that addresses these challenges.

### 3 Preliminaries

Before we develop our Bayesian policy learning framework, we describe the problem setup and notation and provide a brief review of Bayesian policy learning.

#### 3.1 Setup and Notation

We consider an individualized treatment rule or policy, which deterministically maps a set of  $p$  pre-treatment covariates  $\mathbf{X} \in \mathcal{X} \subseteq \mathbb{R}^p$  to a multivalued decision  $D \in \mathcal{D} = \{0, 1, \dots, K - 1\}$  where  $K$  denotes the total number of decision categories. Formally, a policy is defined as a function  $\delta : \mathcal{X} \rightarrow \mathcal{D}$ . We observe a simple random sample of  $n$  observations from the population of interest  $\mathcal{P}$ , which is characterized by the joint distribution of  $\{\mathbf{X}, Y(0), Y(1), \dots, Y(K - 1)\}$  where  $Y(k)$  represents a potential outcome under decision  $D = k$  with  $k \in \mathcal{D}$  and the observed outcome is given by  $Y_i = Y_i(D_i)$  (Neyman, 1923; Rubin, 1974). This notation implicitly assumes no interference between units (Rubin, 1980).

We also assume that the decision is unconfounded given the covariates, i.e.,  $\{Y_i(k)\}_{k=0}^{K-1} \perp\!\!\!\perp D_i \mid \mathbf{X}_i$  (Rosenbaum and Rubin, 1983). However, we do not assume that there exists covariate overlap for treated and controlled units — i.e.,  $0 < \Pr(D_i = k \mid \mathbf{X}_i = \mathbf{x}) < 1$  for all  $k \in \mathcal{D}$  and  $\mathbf{x} \in \mathcal{X}$ . The lack of overlap is motivated by the fact that in many settings, the data are collected under an existing deterministic policy (Dell and Querubin, 2018; Ben-Michael et al., 2021).

Suppose that a policy-maker defines a utility function  $u : \{0, 1, \dots, K - 1\} \times \mathcal{Y} \rightarrow \mathbb{R}$ , which maps every decision-outcome pair to a real-valued utility. Then, the expected utility or value of policy  $\delta$  in a policy class  $\Pi$  is given by,

$$V(\delta) := \mathbb{E}[u(\delta(\mathbf{X}), Y(\delta(\mathbf{X})))]. \quad (1)$$

Our goal is to find an optimal policy within a policy class  $\Pi$  that improves an value upon the existing policy  $\tilde{\delta}$ , which also belongs to the same policy class  $\Pi$  (Ben-Michael et al., 2021; Wei et al., 2022). In our application, the baseline policy is a deterministic rule that produces the security score in the HES. Our goal is to derive a new policy whose average value is higher than that of the original policy subject to a safety constraint introduced in Section 4.

#### 3.2 Bayesian Policy Learning

We next briefly introduce the basic elements of Bayesian policy learning (see Ding and Li, 2018; Li et al., 2022b, for reviews of Bayesian causal inference). Under the Bayesian framework, all parameters are regarded as random variables. Following the convention, we will use upper and lower case characters to represent parameters and their realizations, respectively.

Suppose that the marginal distribution of potential outcomes is characterized by a possibly infinite dimensional parameter  $\Theta$ . Bayesian policy learning proceeds in two steps. First, we specify a prior



distribution  $\pi(\Theta)$  on the parameter  $\Theta$  and compute its posterior distribution using Bayes' rule,

$$\pi(\Theta \mid \{\mathbf{X}_i, D_i, Y_i\}_{i=1}^n) \propto \prod_{i=1}^n p(Y_i \mid \Theta, \mathbf{X}_i, D_i) \pi(\Theta). \quad (2)$$

Under Bayesian policy learning, given the posterior distribution of  $\Theta$ , the optimal policy maximizes the posterior expected value,

$$\delta_{opt} = \operatorname{argmax}_{\delta \in \Pi} \mathbb{E}[V(\delta; \Theta) \mid \{D_i, \mathbf{X}_i, Y_i\}_{i=1}^n], \quad (3)$$

where  $V(\delta; \Theta) := \mathbb{E}[u(\delta(\mathbf{X}), Y(\delta(\mathbf{X}))) \mid \Theta]$ . We explicitly use the notation  $V(\delta; \Theta)$  to emphasize its dependence on the parameter  $\Theta$  as well as the policy  $\delta$ . Specifically,  $V(\delta; \Theta)$  averages over both the marginal distribution of  $\mathbf{X}$ , and the conditional distribution of  $Y(\delta(\mathbf{X}))$  given  $\mathbf{X}$  and  $\Theta$ . The expectation in Equation (3) is taken over the posterior distribution of  $\Theta$  given the observed data.

## 4 The Proposed Methodology

We now describe our Bayesian safe policy learning framework. We begin by introducing a new risk metric, the Average Conditional Risk (ACRisk), that represents the probability that a new policy yields a worse expected utility conditional on covariates than the baseline policy. We then propose to maximize the posterior expected value of the new policy while limiting the posterior expected ACRisk. Our methodology consists of two steps: first estimating the conditional average treatment effect (CATE) using a flexible Bayesian model, and then finding an optimal policy. We formulate this as a chance constraint optimization problem, which in turn can be solved using linear programming based on Markov chain Monte Carlo (MCMC) draws from the posterior distribution of the CATE.

### 4.1 Average Conditional Risk (ACRisk)

In the existing literature, the risk of a policy is typically measured through the estimation uncertainty of its value. To control the risk in policy learning, scholars often seek a policy that has a high value with a small estimation uncertainty. One limitation of this common approach is that it fails to account for potential heterogeneity in risk across different groups of individuals. A policy that performs well on average may not benefit everyone. In our empirical application, a security assessment rule that is effective on average may have a negative impact on some regions. While the risk due to estimation uncertainty will become small as the sample size increases, this inherent risk due to heterogeneous treatment effects will remain, even in large samples.

We introduce a new risk measure, the Average Conditional Risk (ACRisk), to quantify the probability that a policy yields a worse expected utility conditional on the covariates than the baseline policy.

**Definition 1** (Average Conditional Risk (ACRisk)). For a given policy  $\delta$ , the Average Conditional Risk with respect to a baseline policy  $\tilde{\delta}$  is

$$R(\delta, \tilde{\delta}; \theta) := \mathbb{P} \left( \mathbb{E} \left[ u(\delta(\mathbf{X}), Y(\delta(\mathbf{X}))) \mid \mathbf{X}, \Theta = \theta \right] < \mathbb{E} \left[ u(\tilde{\delta}(\mathbf{X}), Y(\tilde{\delta}(\mathbf{X}))) \mid \mathbf{X}, \Theta = \theta \right] \right),$$

	Conditional expected utility		Value	ACRisk
	Group A (50%)	Group B (50%)		
Baseline policy	0	0	0	0
Policy I	4	-2	1	0.5
Policy II	1	1	1	0

Table 1: A numerical example that illustrates the Average Conditional Risk (ACRisk). In this example, both Policies I and II outperform the baseline policy on average, but the improvement of Policy I comes at the expense of the group B. The ACRisk shows that 50% of the population, which is the size of the group  $B$  in this example, is at risk.

where  $\Theta$  represents the possibly infinite-dimensional parameter that governs the marginal distributions of potential outcomes.

The inner expectation in the definition of the ACRisk is taken over the conditional distribution of  $Y(\delta(\mathbf{X}))$  given  $\mathbf{X}$  and  $\Theta$  while the outer probability is with respect to the marginal distribution of  $\mathbf{X}$ . We use the above notation to make it explicit that the ACRisk depends on the parameter  $\Theta$ , which governs the conditional distribution of potential outcomes given the covariates  $\mathbf{X}$ . Note that under this definition,  $R(\tilde{\delta}, \tilde{\delta}; \theta) = 0$  for any value of  $\theta$ .

Intuitively, the ACRisk first evaluates whether a group of individuals with a certain set of covariates has a lower expected utility under policy  $\delta$  than under the baseline policy  $\tilde{\delta}$ . It then computes the proportion of such “at risk” groups in the population by averaging over the distribution of covariates. The ACRisk is dependent on the covariates we choose, and using different set of covariates can result in different “at risk” groups, potentially leading to different ACRisk values.

Table 1 provides a numerical example where both Policies I and II outperform the baseline policy. While the improvement of Policy I comes at the expense of group B, Policy II performs equally well for both groups. As a result, the ACRisk of Policy I is higher, indicating that 50% of the population is at risk.

We note that the ACRisk is a risk measure based on groups (defined by covariates  $X$ ). In particular, the ACRisk differs from the following individual measure of risk.

**Definition 2** (Average Individual Risk (AIRisk)). For a given policy  $\delta$ , its average individual risk with respect to a baseline policy  $\tilde{\delta}$  is defined as,

$$R^*(\delta, \tilde{\delta}; \lambda) := \mathbb{P} \left( u(\delta(\mathbf{X}), Y(\delta(\mathbf{X}))) < u(\delta(\mathbf{X}), Y(\tilde{\delta}(\mathbf{X}))) \mid \Lambda = \lambda \right),$$

where  $\Lambda$  represents a (possibly infinite dimensional) parameter that governs the joint distribution of potential outcomes.

Unlike the ACRisk, the AIRisk is not identifiable because it depends on the joint distribution of potential outcomes. One possible strategy is to control an upper bound of the AIRisk (Kallus, 2022; Ben-Michael et al., 2022; Li et al., 2022a). We leave the development of safe policy learning in terms of the AIRisk to future research and focus on the ACRisk for the remainder of this paper.

To control the ACRisk, we must estimate the parameter  $\Theta$ . Under our Bayesian safe policy learning framework, we consider the posterior average of the ACRisk, which we call the Posterior Average Conditional Risk or PACRisk. This measure allows us to incorporate the estimation uncertainty into our analysis.

**Definition 3** (Posterior Average Conditional Risk (PACRisk)). For a given policy  $\delta$ , the Posterior Average Conditional Risk with respect to a baseline policy  $\tilde{\delta}$  is

$$R_p(\delta, \tilde{\delta}) := \mathbb{E} \left[ R(\delta, \tilde{\delta}; \Theta) \mid \{D_i, \mathbf{X}_i, Y_i\}_{i=1}^n \right],$$

where the expectation is taken over the posterior distribution of  $\Theta$  given the observed data  $\{D_i, \mathbf{X}_i, Y_i\}_{i=1}^n$ .

## 4.2 Bayesian Safe Policy Learning with Chance Constraint Optimization

We now propose a Bayesian safe policy learning procedure that limits the PACRisk introduced above (Definition 3). Specifically, we find a policy within a policy class  $\Pi$  that maximizes the posterior average value while limiting the PACRisk below a specified threshold  $\epsilon \in [0, 1]$ ,

$$\delta_{\text{safe}} = \underset{\delta \in \Pi}{\operatorname{argmax}} \mathbb{E} [V(\delta; \Theta) \mid \{D_i, \mathbf{X}_i, Y_i\}_{i=1}^n] \quad \text{subject to} \quad R_p(\delta, \tilde{\delta}) \leq \epsilon. \quad (4)$$

The expectation in the optimization target is taken over the posterior distribution of the parameter  $\Theta$ . We typically choose a policy class  $\Pi$  that contains the baseline policy so that a solution to Equation (4) always exists.

For intuition on this procedure, imagine randomly selecting an individual from the population. The constraint in Equation (4) ensures that  $\delta_{\text{safe}}$  has an at most  $\epsilon$  posterior probability of yielding a worse expected value for the group of individuals with the same characteristics as the randomly selected individual. Thus, a smaller value of  $\epsilon$  yields a safer policy that is more conservative, limiting the extent of changes to the baseline policy.

By plugging in the definition of the PACRisk (Definition 3), the Bayesian safe policy learning problem in Equation (4) can be equivalently written as the following chance-constrained optimization problem:

$$\begin{aligned} \delta_{\text{safe}} = \underset{\delta \in \Pi}{\operatorname{argmax}} \quad & \mathbb{E} [V(\delta; \Theta) \mid \{D_i, \mathbf{X}_i, Y_i\}_{i=1}^n] \\ \text{subject to} \quad & \mathbb{P} \left( u(\delta(\mathbf{X}), Y(\delta(\mathbf{X}))) < u(\delta(\mathbf{X}), Y(\tilde{\delta}(\mathbf{X}))) \mid \{D_i, \mathbf{X}_i, Y_i\}_{i=1}^n \right) \leq \epsilon, \end{aligned} \quad (5)$$

where the probability in the constraint is taken over the distribution of  $\mathbf{X}$  and the posterior distribution of  $\Theta$ .

Policy optimization problems with a chance constraint involving the posterior distribution of  $\Theta$  are difficult to solve in general with a sampling-based approach. Although we can use posterior draws of  $\Theta$  to evaluate the chance constraint, they do not provide information about how the value of the constraint changes as a function of the policy  $\delta$  (see [Delage and Mannor, 2010](#), for a similar optimization problem). Therefore, researchers typically impose strong assumptions on the marginal distribution of

potential outcomes and the parameter  $\Theta$  to obtain a closed-form solution (e.g., [Delage and Mannor, 2010](#); [Vitus et al., 2015](#); [Mowbray et al., 2022](#)).

We overcome this challenge by formulating the optimization problem given in Equation (5) as a constrained linear programming problem that separates the parameter  $\Theta$  and the policy  $\delta$ . In this way, the proposed Bayesian safe policy learning procedure can be conducted in two steps, First, we use flexible Bayesian models to obtain posterior samples of  $\Theta$  and write the corresponding chance constraint (5) as a function of policy  $\delta$ . We then conduct policy optimization based on the given criteria. The following theorem formally establishes the equivalence between the chance constraint optimization in Equation (5) and a constrained linear programming problem.

**Theorem 1** (Bayesian Safe Policy Learning as a Linear Programming Problem). Define the posterior conditional benefit and risk of decision  $k$  relative to the existing policy  $\tilde{\delta}$  as,

$$\begin{aligned} b_k(\mathbf{x}) &:= \mathbb{E}[\tau_k(\mathbf{x}, \Theta) \mid \{D_i, \mathbf{X}_i, Y_i\}_{i=1}^n], \\ r_k(\mathbf{x}) &:= \mathbb{P}(\tau_k(\mathbf{x}, \Theta) < 0 \mid \{D_i, \mathbf{X}_i, Y_i\}_{i=1}^n), \end{aligned}$$

where  $\tau_k(\mathbf{x}, \theta) := \mathbb{E}[u(k, Y(k)) - u(\tilde{\delta}(\mathbf{x}), Y(\tilde{\delta}(\mathbf{x}))) \mid \mathbf{X} = \mathbf{x}, \Theta = \theta]$ . Then, the chance-constraint optimization defined in Equation (5) is equivalent to the following constrained linear programming problem,

$$\begin{aligned} \delta_{\text{safe}} &= \underset{\delta \in \Pi}{\operatorname{argmax}} \sum_{k=0}^{K-1} \int I(\delta(\mathbf{X}) = k) b_k(\mathbf{X}) dF(\mathbf{X}) \\ &\text{subject to } \sum_{k=0}^{K-1} \int I(\delta(\mathbf{X}) = k) r_k(\mathbf{x}) dF(\mathbf{X}) \leq \epsilon \end{aligned} \tag{6}$$

where  $F(\mathbf{x})$  is the cumulative distribution function of covariates  $\mathbf{X}$ .

Proof is given in Appendix S3. In the statement of the theorem,  $\tau_k(x, \theta)$  represents an improvement in the conditional expected utility when changing the decision  $\tilde{\delta}(x)$  to  $k$  where  $\{\tau_k(x, \Theta)\}_{k=0}^{K-1}$  is fully determined by  $K - 1$  pairwise CATEs between  $K$  decisions.

Theorem 1 enables us to approximate the conditional improvement and risk, i.e.,  $b_k(\mathbf{x})$  and  $r_k(\mathbf{x})$ , using posterior draws and convert the original chance-constrained optimization problem into a deterministic one. This formulation is possible because the ACRisk of a policy  $\delta$  is a weighted average of its conditional risk given  $\mathbf{X}$ , which can be represented by  $\{r_k(\mathbf{x})\}_{k=0}^{K-1}$ . Therefore, we can first compute the conditional risk, i.e.,  $r_k(\mathbf{x})$ , and the conditional improvement over the baseline policy, i.e.,  $b_k(\mathbf{x})$ , and then optimize over the policies.

If we use the empirical distribution of  $X$  for  $F(\mathbf{X})$  i.e.,  $F_n(\mathbf{x}) = \frac{1}{n} \sum_{i=1}^n I(x \leq \mathbf{X}_i)$ , the number of decision variables will be equal to the number of observations. In this case, the optimization problem given in Equation (6) will become an integer linear programming problem with the following linear

---

**Algorithm 1:** Bayesian Safe Policy Learning

---

**Input:** Data  $\{D_i, \mathbf{X}_i, Y_i\}_{i=1}^n$ ; A total of  $M$  posterior draws, i.e.,  $\{\Theta^{(m)}\}_{m=1}^M$ ; Covariate distribution function  $F(x)$

**Output:** Bayesian safe policy  $\hat{\delta}_{\text{safe}} : \mathcal{X} \rightarrow \mathcal{D} = \{0, 1, \dots, K-1\}$

- 1 Approximate the posterior conditional benefit of decision  $k$ ,

$b_k(\mathbf{x}) = \mathbb{E}[\tau_k(\mathbf{x}, \Theta) \mid \{D_i, \mathbf{X}_i, Y_i\}_{i=1}^n]$ , by the sample average of posterior draws for  $\mathbf{x} \in \mathcal{X}$ :

$$\hat{b}_k(\mathbf{x}) = \frac{1}{M} \sum_{m=1}^M \tau_k(\mathbf{x}, \Theta^{(m)})$$

- 2 Approximate the posterior conditional risk of decision  $k$ .

$r_k(\mathbf{x}) = \mathbb{P}(\tau_k(\mathbf{x}, \Theta) < 0 \mid \{D_i, \mathbf{X}_i, Y_i\}_{i=1}^n)$ , by the sample average of posterior draws for  $\mathbf{x} \in \mathcal{X}$ :

$$\hat{r}_k(\mathbf{x}) = \frac{1}{M} \sum_{m=1}^M I\{\tau_k(\mathbf{x}, \Theta^{(m)}) < 0\}$$

- 3 Solve this approximated optimization problem:

$$\begin{aligned} \hat{\delta}_{\text{safe}} &= \operatorname{argmax}_{\delta \in \Pi} \sum_{k=0}^{K-1} \int I(\delta(\mathbf{X}) = k) \hat{b}_k(\mathbf{X}) dF(\mathbf{X}) \\ \text{subject to} & \sum_{k=0}^{K-1} \int I(\delta(\mathbf{X}) = k) \hat{r}_k(\mathbf{x}) dF(\mathbf{X}) \leq \epsilon \end{aligned}$$

---

constraint, which can be efficiently solved by a numerical optimization package such as Gurobi.

$$\begin{aligned} \hat{\delta}_{\text{safe}} &= \operatorname{argmax}_{\delta \in \Pi} \frac{1}{n} \sum_{i=1}^n \sum_{k=0}^{K-1} I(\delta(\mathbf{X}_i) = k) \hat{b}_k(\mathbf{X}_i) \\ \text{subject to} & \frac{1}{n} \sum_{i=1}^n \sum_{k=0}^{K-1} I(\delta(\mathbf{X}_i) = k) \hat{c}_k(\mathbf{X}_i) \leq \epsilon. \end{aligned} \tag{7}$$

Further restrictions on  $\delta$  via the policy class  $\Pi$  can also be incorporated; we discuss details in the simulation study (Section 5) and the empirical analysis (Section 6). Algorithm 1 summarizes the procedure for Bayesian safe policy learning with posterior draws of  $\Theta$ .

### 4.3 Use of Bayesian Nonparametric Models

A primary advantage of the proposed Bayesian safe policy learning framework introduced above is the separation of CATE estimation and policy optimization. This means that our framework can readily accommodate the use of flexible Bayesian nonparametric models for estimating the CATE. Here, we demonstrate this advantage by considering two commonly used models, i.e., Bayesian Additive Regression Trees (BART) and Gaussian Processes (GP), for Bayesian causal inference (Hill, 2011; Branson et al., 2019). Although the framework introduced in Section 4.2 is completely general, below

we apply it to a concrete example to demonstrate how the framework can be used in practice.

As an example that mirrors our empirical application, suppose that we have an ordered decision,  $k \in \{0, 1, \dots, K - 1\}$  and a continuous outcome. We begin by modeling the marginal distribution of the baseline potential outcome  $Y_i(0)$  and then the  $K - 1$  CATEs between two adjacent treatment levels. Specifically, we assume the following model,

$$Y_i(k) = \sum_{d=0}^k f_d(X_i) + \epsilon_i, \quad \forall k \in \{0, 1, \dots, K - 1\} \quad (8)$$

where  $\epsilon_i$  are i.i.d Gaussian noise with mean 0 and variance  $\sigma^2$ ,  $f_0(\mathbf{x}) = \mathbb{E}[Y(0) \mid \mathbf{X} = \mathbf{x}]$ , and  $f_k(\mathbf{x}) = \mathbb{E}[Y(k) - Y(k - 1) \mid \mathbf{X} = \mathbf{x}]$  for  $1 \leq k \leq K - 1$ . Here, we have an infinite dimensional parameter  $\Theta = \left(\sigma^2, \{f_k(\cdot)\}_{k=0}^{K-1}\right)$  that determines the marginal distribution of each potential outcome  $Y(k)$  given covariates  $\mathbf{X}$ . If we have binary or categorical outcomes, we use a link function to transform the mean outcome to a continuous scale.

Below, we consider BART and GP for Bayesian inference on these parameters  $\{f_k\}_{k=0}^{K-1}$ . Specifically, we sample from the posterior distribution of  $\{f_k\}_{k=0}^{K-1}$  and apply Algorithm 1 to drive a safe policy.

**Bayesian Additive Regression Trees (BART).** BART is a popular Bayesian nonparametric model that is commonly used for causal inference, especially to estimate the CATE (Taddy et al., 2016; Hahn et al., 2020). In general, BART excels in learning complex nonlinear relations while it is often poor at extrapolating. Thus, it is suitable when there exists a substantial covariate overlap between treatment conditions.

We separately fit BART to model each  $f_k$  for  $k \in \{0, 1, \dots, K - 1\}$  as the sum of  $L$  regression trees, i.e.,  $f_k(\mathbf{x}) = \sum_{\ell=1}^L g_{k\ell}(\mathbf{x}; T_{k\ell}, P_{k\ell})$  where  $g_{k\ell}(\cdot)$  is the  $\ell$ -th regression tree with parameter  $T_{k\ell}$  and  $P_{k\ell}$  denoting the structure of the regression tree and the parameters in the terminal nodes, respectively. Thus, the parameter  $\Theta$  consists of  $\{T_{k\ell}, P_{k\ell}\}_{1 \leq \ell \leq L, 0 \leq k \leq K-1}$  as well as  $\sigma^2$ . We draw posterior samples for  $\{T_{k\ell}, P_{k\ell}\}_{1 \leq \ell \leq L}$  using an MCMC algorithm once a prior distribution is specified (Chipman et al., 2010).

**Gaussian Process Regression.** Another popular Bayesian nonparametric model is Gaussian Process regression (GP). GP has a greater degree of smoothness than BART, making it more suitable for extrapolation (Rasmussen and Williams, 2006; Branson et al., 2019). Therefore, we should consider using GP when the overlap of covariates between treatment conditions is poor.

As in the case of BART, we separately fit GP to model each  $f_k$ . Specifically,  $f_k$  is assumed to be a random function based on a collection of Gaussian processes. To conduct Bayesian inference on  $f_k$ , we specify a prior for  $f_k$  by giving the mean function  $\mu_k(\cdot)$  and kernel function  $K_k(\cdot, \cdot)$  and obtain posterior samples of  $f_k$  using the MCMC algorithm (Rasmussen and Williams, 2006; Branson et al., 2019).

When strong prior information is unavailable, we can set  $\mu_k(\cdot) = 0$  for  $k \geq 1$  which corresponds to no treatment effect. For the kernel function, which determines the covariance between  $f_k(\mathbf{x}_1), f_k(\mathbf{x}_2)$

for any  $\mathbf{x}_0, \mathbf{x}_1 \in \mathcal{X}$ , common choices are the Squared Exponential and Matern kernels:

$$K_{SE}(\mathbf{x}_1, \mathbf{x}_2) = \sigma_0^2 \exp\left(-\frac{\|\mathbf{x}_1 - \mathbf{x}_2\|^2}{2\ell}\right) \quad (9)$$

$$K_{\text{Matern}}(\mathbf{x}_1, \mathbf{x}_2) = \sigma_0^2 \frac{2^{1-\nu}}{\Gamma(\nu)} \left(\frac{\sqrt{2\nu}\|\mathbf{x}_1 - \mathbf{x}_2\|}{\ell}\right)^\nu B_\nu\left(\frac{\sqrt{2\nu}\|\mathbf{x}_1 - \mathbf{x}_2\|}{\ell}\right) \quad (10)$$

where  $\ell$  is the scale parameter,  $\sigma_0^2$  is the variance parameter,  $B_\nu$  is the modified Bessel function of the second kind, and  $\nu$  is the smoothness parameter. The hyperparameters in the Squared Exponential and Matern kernels can be selected based on prior knowledge about the smoothness of  $f_k(\cdot)$ . For example, to make  $f_k$  more smooth, we can increase the scale and smoothness parameters. In general,  $\ell$  and  $\nu$  determine the prior knowledge about the smoothness of  $f$ , while  $\sigma_0^2$  determines the strength of the prior knowledge.

Extrapolation based on GP is similar to frequentist extrapolation methods that specify the model class by assuming a certain type of smoothness on the CATE under the robust optimization framework. For example, [Ben-Michael et al. \(2021\)](#) considers the case with two arms and assumes a Lipschitz constraint on the CATE, i.e.,  $|f_1(\mathbf{x}_1) - f_1(\mathbf{x}_2)| \leq c\|\mathbf{x}_1 - \mathbf{x}_2\|$ . In our framework, if we specify the prior of  $f_1(\mathbf{x})$  as a GP with mean function  $m(\mathbf{x})$  that is  $c_1$  Lipschitz, then the Squared Exponential kernel with scale parameter  $\ell$  implies a  $c_2$  probabilistic Lipschitz condition on  $f_1(\mathbf{x})$ ,

$$\mathbb{P}(|f_1(\mathbf{x}_1) - f_1(\mathbf{x}_2)| > c_2\|\mathbf{x}_1 - \mathbf{x}_2\|) \leq \sigma_0^2 \left(\frac{1}{c_2^2 \ell^2} + \frac{c_1^2}{c_2^2}\right)$$

Similarly, the Matern kernel with scale parameter  $\ell$  and smoothness parameter  $\nu$  implies the following probabilistic Lipschitz condition:

$$\mathbb{P}(|f_1(\mathbf{x}_1) - f_1(\mathbf{x}_2)| > c_2\|\mathbf{x}_1 - \mathbf{x}_2\|) \leq \sigma_0^2 \left\{ \left(1 + \frac{1}{\nu - 1}\right) \frac{1}{c_2^2 \ell^2} + \frac{c_1^2}{c_2^2} \right\}$$

Thus, there exists a direct relation between the prior hyperparameter of GP and the smoothness of the underlying model.

## 5 A Simulation Study

In this section, we conduct a simulation study to examine the empirical performance of the proposed Bayesian safe policy learning methodology. To highlight the key concepts, we consider a simple setup with a binary decision.

### 5.1 Setup

We consider the following data generating processes with the number of observations  $n$  varying from 50 to 500, i.e.,  $n \in \{50, 100, 200, 500\}$ . There are two covariates  $\mathbf{X} = (X_1, X_2)$  that are independently and identically distributed according to a uniform distribution  $X_1, X_2 \stackrel{i.i.d.}{\sim} \text{Uniform}(-1, 1)$ . We consider the following two scenarios, one with covariate overlap and the other without it:



- **Scenario I (with covariate overlap):** The data are collected through a randomized experiment with  $\mathbb{P}(D = 1 \mid \mathbf{X} = \mathbf{x}) = 0.5, \forall \mathbf{x} \in \mathcal{X}$ . Here, the baseline policy is not to give anyone the treatment, i.e.,  $\tilde{\delta}(\mathbf{x}) = 0, \forall \mathbf{x} \in \mathcal{X}$ .
- **Scenario II (without covariate overlap):** The data are collected under a deterministic policy  $\tilde{\delta}(x) = I(x_1 > 0.5)$ , which serves as the baseline policy. Thus, the treatment assignment is also deterministic, i.e.,  $\mathbb{P}(D = 1 \mid \mathbf{X} = \mathbf{x}) = \tilde{\delta}(\mathbf{x})$ .

Within each simulation scenario, we specify the outcome model as,<sup>3</sup>

$$Y \mid \mathbf{X} \sim N \left( X_1 + X_2 + \{4I(X_1 > 0, X_2 > 0) - 2\}D \mid X_1 \mid \mid X_2 \mid, \sigma^2 \right)$$

where we consider a high signal-to-noise ratio case ( $\sigma = 1$ ), a medium signal-to-noise ratio case ( $\sigma = 2$ ), and a low signal-to-noise ratio case ( $\sigma = 3$ ). In this setup, treatment is effective for individuals with  $X_1 > 0, X_2 > 0$ . Finally, we set the utility to be equal to the outcome, i.e.,  $u(d, y) = y$ .

We consider policies based on a linear separation of the covariate space  $\mathcal{X}$ :

$$\Pi := \{ \delta(\cdot, \cdot) : \delta(x_1, x_2) = I(ax_1 + bx_2 + c > 0); a, b, c \in \mathbb{R} \} \quad (11)$$

Notice that this policy class does not contain the oracle treatment rule — giving the treatment to individuals with  $X_1 > 0$  and  $X_2 > 0$ .

For Scenario I with covariate overlap, we use Bayesian Causal Forest (BCF) to estimate the CATE and the expected outcome under the control condition, i.e.,  $\mathbb{E}(Y(0))$ , with the default hyperparameter specification suggested by [Hahn et al. \(2020\)](#). For modeling  $\mathbb{E}[Y(0) \mid \mathbf{X}]$ , we use 200 trees and hyperparameters of  $\beta = 2, \eta = 0.95$ . For modeling the CATE, we impose a stronger prior and use a BART model with 50 trees, and  $\beta = 3, \eta = 0.25$ .

For Scenario II without covariate overlap, we use Gaussian Process regression (GP) to model the expected outcome under the control condition as well as the CATE. We set the kernel of the Gaussian process as a Matern kernel with parameter  $l = 0.5, 1$  or  $2, \nu = 3/2$  (see Equation (10)). We use a non-informative prior where the mean function of the GP,  $m(x)$ , is set to 0. For other hyperparameters in the kernel function, we set the length scale to  $\{0.5, 1, 2\}$  which correspond to a *not smooth*, *medium smooth*, and *very smooth* CATE. We set  $\sigma_0^2$  to  $\{1, 4, 16\}$  which corresponds to a *strong*, *medium*, and *weak* prior.

For both methods, we use `Stan` ([Carpenter et al., 2017](#)) to compute 2,000 posterior samples from two chains with a burn-in period of 500 samples.

## 5.2 Findings

We first investigate how the value and ACRisk of the safe policy changes as a function of the safety constraint  $\epsilon$  in Equation (4) under the different data-generating processes described above. We then

<sup>3</sup>We also consider a data generating process with binary outcomes in Appendix S4. The results are broadly similar to the continuous case.

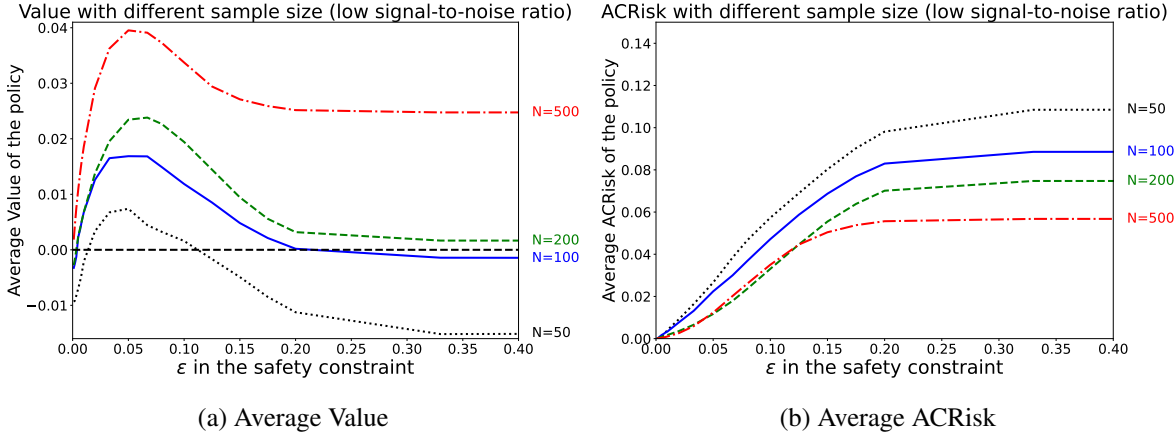


Figure 3: Average Value and ACRisk for learned policies using data with covariate overlap, varying the safety constraint and sample size.

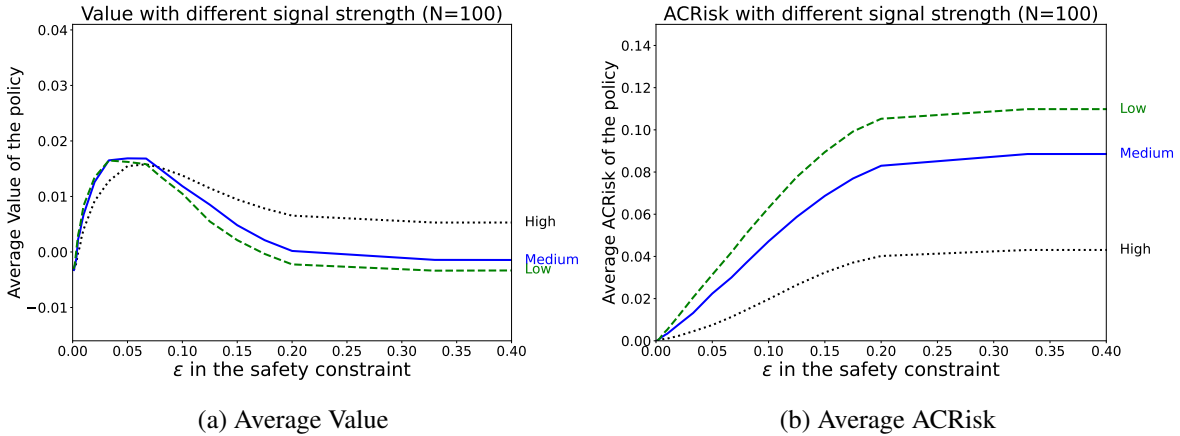


Figure 4: Average Value and ACRisk for learned policies using data with covariate overlap, varying the safety constraint and signal strength.

examine the influence of the prior distribution on the performance of the proposed methodology when there is no covariate overlap.

**Sample size and signal strength.** Figure 3 presents the average value and average ACRisk for learned policies under different values of the safety constraint  $\epsilon$  ( $x$ -axis) with various sample sizes, using the continuous outcome model. Figure 4 shows the results with different signal-to-noise ratios, using the continuous outcome model. In both figures, the results are generated under Scenario I, and so there is no extrapolation. As expected, we find that a weaker of safety constraint (i.e., a larger value of  $\epsilon$ ) leads to a greater ACRisk of the learned policy, reaching to a plateau corresponding to the ACRisk of the policy obtained by maximizing the posterior expected utility without a constraint.

On average, a smaller sample size and smaller signal-to-noise ratio lead to a greater ACRisk. Interestingly, an appropriate level (e.g., around 0.05 in this simulation) of the safety constraint achieves a greater average value compared to having no safety constraint and purely maximizing the posterior

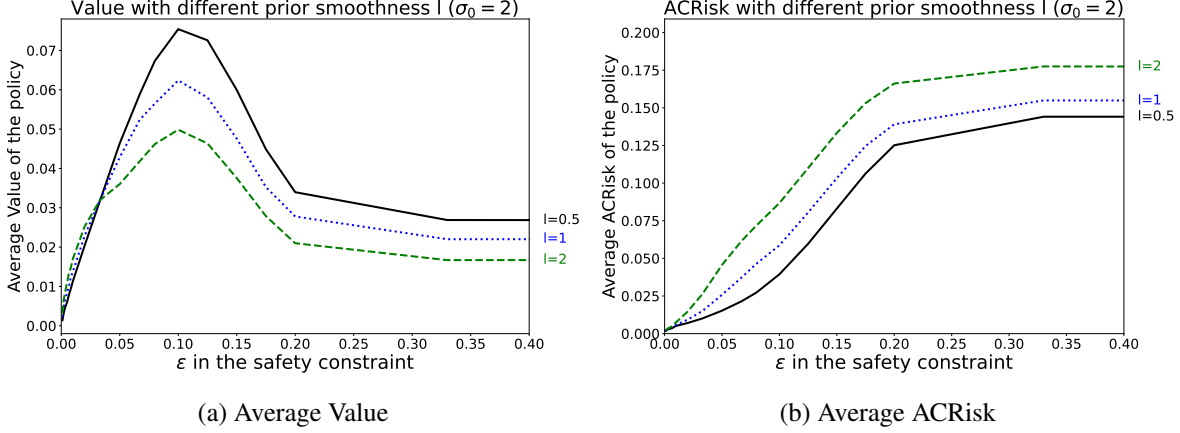


Figure 5: Average Value and ACRisk for learned policies using data without covariate overlap, varying the safety constraint and prior smoothness for the CATE.

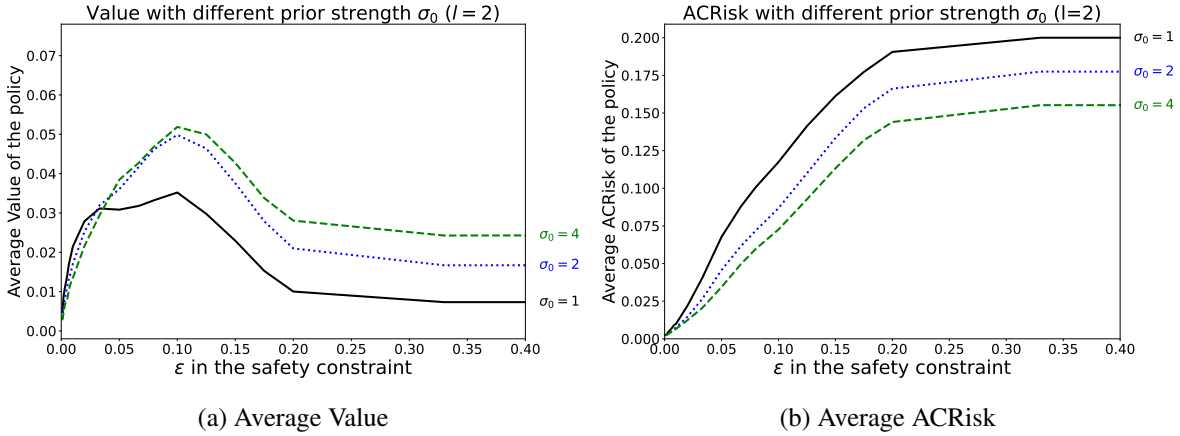


Figure 6: Average Value and ACRisk for learned policies using data without covariate overlap, varying the safety constraint and prior strength for the CATE.

expected value. This is especially true when the sample size and/or the signal-to-noise ratio is small. In such settings, the safety constraint regularizes the policy optimization, only modifying the existing policy for those who are expected to benefit from a new policy with a high degree of certainty.

**Prior in extrapolation.** Next, we investigate the influence of prior parameters in GP on the performance of the proposed methodology under Scenario II of no covariate overlap. Specifically, we consider the scale parameter  $l$  and the variance parameter  $\sigma_0^2$ , which determine the smoothness of the CATE and the prior strength, respectively. Recall that a greater value of  $l$  implies a smoother function, while a smaller value of  $\sigma_0^2$  corresponds to a stronger belief in the prior information. Given a space constraint, we fix the sample size to 200 and use a low signal-to-noise ratio when generating the data.

Figures 5a and 6a show the average value of the learned policy under different prior smoothness and strength. In general, the value of learned policy tends to decrease as the prior smoothness and strength increase. However, when the safety constraint is very strong (i.e.,  $\epsilon$  is small), the value of the

learned policy with a stronger or smoother prior is slightly greater. This is because a very small  $\epsilon$  means that we only want to change the baseline policy on the group of covariates with the most significant treatment effects. A stronger or smoother prior leads to a more conservative estimation of the CATE and can better identify such group of covariates. In terms of the average ACRisk, Figure 5b shows that as the prior for the CATE becomes smoother, we extrapolate further, leading to an increase in the average ACRisk. Figure 6b shows a similar pattern where the average ACRisk increases as the prior becomes stronger.

To summarize, our simulation study shows that the safety constraint on the PACRisk can effectively control the true ACRisk in policy learning, reducing the risk of harming specified subgroups. In addition, a moderately binding safety constraint can induce beneficial regularization and improve the average value of the learned policy, especially when the sample size and signal strength are small.

## 6 Empirical Analysis of the HES Security Assessment

With our methodological development in hand, we now return to analyzing the military security assessment described. As we discussed in Section 2, we will focus on learning a new rule to aggregate the 20 sub-model scores into one overall security score, while keeping the original structure of the HES by only modifying the two-way and three-way tables used for the aggregation.

### 6.1 Setup

To formalize our problem, let  $X^{(k)} \in [1, 5]$  denote the  $k$ -th sub-model scores with  $k \in \{1, 2, \dots, 20\}$ , where  $\mathbf{X} \in \mathcal{X}$  denotes the whole 20-dimensional input vector. We use  $S^{(i,j)} \in \{1, 2, 3, 4, 5\}$  to represent the  $i$ th score at the  $j$ th level where  $i \in \{1, 2, \dots, n_j\}$  and  $j \in \{1, 2, 3\}$  with  $n_j$  representing the total number of scores aggregated at the  $j$ -th level. We note that  $X^{(k)} \neq S^{(1,k)}$  because the raw input score  $X^{(k)}$  is rounded to obtain the first level score  $S^{(1,k)}$ .

The output security score is denoted by  $D \in \mathcal{D} = \{1, 2, 3, 4, 5\}$ . We use  $Y \in \{0, 1\}$  to represent one of three binary regional development outcomes measured in January, 1970: *regional safety*, *regional economy*, and *regional civic society* separately in the analysis. These variables are calculated in Dell and Querubin (2018) with a latent class analysis on data from the HES, armed forces administrative records, and public opinion surveys.

We consider a policy  $\delta$ , which is a deterministic function mapping the inputs  $\mathbf{x} \in \mathcal{X}$  (the 20 sub-model scores) to an output score  $d \in \mathcal{D}$ . We define two-way and three-way decision tables as the following functions that map integer-valued input scores to an integer-valued output score. Recall that each input/output score takes an integer value, ranging from 1 to 5.

$$\begin{aligned} T_2(\cdot, \cdot) &: \{1, 2, 3, 4, 5\}^2 \rightarrow \{1, 2, 3, 4, 5\}, \\ T_3(\cdot, \cdot, \cdot) &: \{1, 2, 3, 4, 5\}^3 \rightarrow \{1, 2, 3, 4, 5\}. \end{aligned} \tag{12}$$

Let  $\tilde{T}_2$  and  $\tilde{T}_3$  represent the baseline decision tables used in the existing HES. These existing rules are *monotonic*, meaning that a decision table with a greater input score never yields a smaller output score, holding the other input scores constant. Formally, a two-way decision table  $T_2$  is monotonic if

and only if  $\forall i_1, j_1, i_2, j_2 \in \{1, 2, 3, 4, 5\}$  and  $i_1 \leq i_2, j_1 \leq j_2, T_2(i_1, j_1) \leq T_2(i_2, j_2)$ . Similarly, a three-way decision table  $T_3$  is monotonic if and only if  $\forall i_1, j_1, k_1, i_2, j_2, k_2 \in \{1, 2, 3, 4, 5\}$  and  $i_1 \leq i_2, j_1 \leq j_2, k_1 \leq k_2, T_3(i_1, j_1, k_1) \leq T_3(i_2, j_2, k_2)$ . This condition is reasonable in our context because higher submodel scores should not make a region less secure. We will require that our learned decision tables also satisfy this monotonicity condition.

## 6.2 Learning to the aggregate military, economic, and political sub-models

We begin by learning a single decision table while keeping the other existing tables used in the HES. In particular, we consider learning a new third-level three-way decision table  $T_3$  that aggregates three scores in the third level — the Military, Political, and Social Economic models — and produces the final output security score  $D$  (see Figure 1).

We use separate GPs with a logit link function  $g$  to model the expected outcome under different decisions (see Section 4.3). Specifically, we assume

$$Y_i(d) \mid \mathbf{X}_i \sim \text{Bernoulli}(p_d(\mathbf{X}_i)) \text{ where } p_d(\mathbf{X}_i) = g^{-1} \left( \sum_{k=1}^d f_{k-1}(\mathbf{X}_i) \right) \quad (13)$$

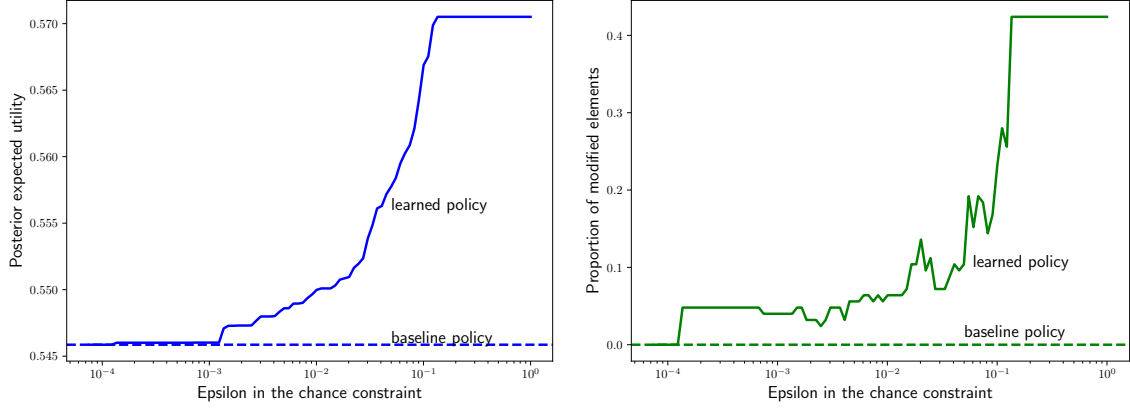
for  $d = 1, 2, 3, 4, 5$ . Here,  $f_0$  is used to model the expected outcome under the decision  $D = 1$ , whereas  $\{f_k\}_{k=1}^4$  are used to model the effect between two adjacent decisions.

We set the prior mean function for all the GPs to zero, i.e.,  $m(x) = 0$ , implying that all potential outcomes are distributed as Bernoulli with probability  $1/2$ . For the kernel function of the GP, we use a Matern kernel with  $\nu = 3/2, l = 1, \sigma_0^2 = 4$  (see Equation (10)). This corresponds to a very weak prior which implies with more than 90% probability,  $f_k(\cdot)$  is no less smooth than a Lipschitz function with the Lipschitz constant 10.95.

Given the small size of the optimization problem when optimizing a single decision table, we use the Gurobi solver to optimize Equation (4) over three-way monotonic decision tables. We use the military impacts on regional *safety*, *economy*, and *civic society* as separate binary outcomes and let the utility function equal  $u(D, Y) = Y$ .

Figure 7 shows how the results of our Bayesian safe policy learning procedure change with the safety constraint  $\epsilon$  when the outcome is regional *safety*. Figure 7a shows the posterior expected utility of the learned policy, while Figure 7b presents the proportion of changed elements in the three-way table. We find that a weaker safety constraint (i.e., a greater value of  $\epsilon$ ) leads to a greater difference between the learned and baseline policies in terms of the three-way table. The learned policy also has a higher posterior expected utility when the safety constraint is weaker.

Figure 8 presents the relative difference in the partial dependence (PD) between the baseline and learned policies, with respect to the three level-3 scores. The PD function measures the dependence of the output security score on the level-3 scores  $S^{(3,1)}, S^{(3,2)}, S^{(3,3)}$  by computing the marginal expected output of the policy given certain input scores (Friedman, 2001; Greenwell et al., 2018). For example,



(a) Posterior expected utility of the learned policy. (b) Proportion of elements in the three-way table changed by the learned policy.

Figure 7: The posterior expected utility of the learned policy (a) and the proportion of elements in the three-way table changed by the learned policy (b) under different values of  $\epsilon$ , when regional *safety* development is the outcome. A weaker safety constraint (i.e., a greater value of  $\epsilon$ ) leads to a greater difference between the baseline and learned policies. The posterior expected utility also becomes greater.

the PD function for policy  $\delta(\cdot; T_3)$  with respect to level-3 military score  $S^{(3,1)}$  is computed as,

$$I_{military}(x; T_3) = \frac{1}{n} \sum_{i=1}^n T_3(x, S_i^{(3,2)}, S_i^{(3,3)}). \quad (14)$$

We find the percent change in the PD function between the learned and baseline policies are mostly positive, meaning that the expected output security score under the learned policy is generally higher than the baseline policy for all three level-3 input scores. This finding is consistent with that of [Dell and Querubin \(2018\)](#): airstrikes increased the military and political activities of the communist insurgency, decreasing regional safety and economy. Since a higher security score signifies a safer region, it is likely to decrease the frequency of airstrikes, and potentially improve the regional outcome.

We further compute the PD importance ([Greenwell et al., 2018](#)) of the military, political, and socioeconomic level-3 scores under the learned policy as a function of the safety constraint  $\epsilon$ , using the three different outcomes. The PD importance measures how flat the PD function is and a flat PD function leads to a small PD importance, meaning that the output score is not sensitive to the input. For ease of interpretation, we scale the PD importance of level-3 scores for each policy so that they sum to one, allowing us to compare the PD importance of level-3 scores across different policies.

Figure 9 compares the scaled PD importance of each factor (denoted by different colors) between the baseline (dotted lines) and learned (solid lines) policies as a function of the strength of the safety constraint  $\epsilon$ . The figure shows a consistent pattern where the new learned policies upweight the socioeconomic model and downweight the military model. This is true when targeting both economic and civic society outcomes (Figures 9a and 9b), as we may expect, but it is also the case when targeting

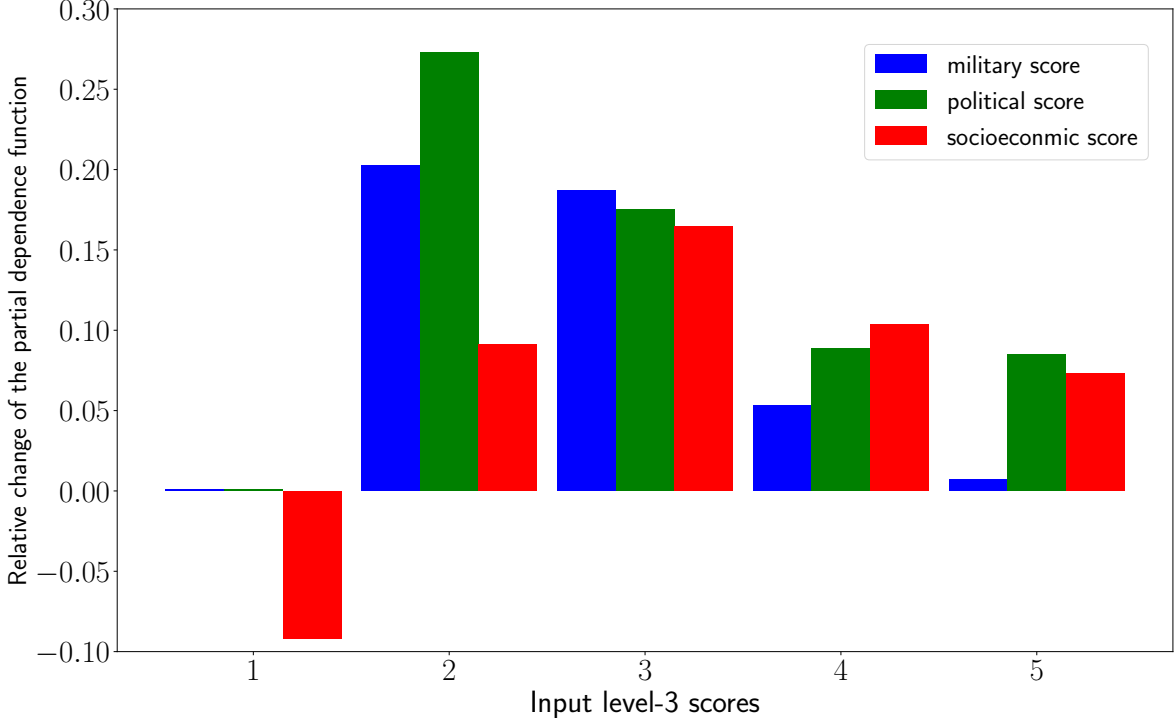


Figure 8: The relative change of the PD function from the baseline policy to the learned policy for  $\epsilon = 0.1$ . Each block corresponds to the different input of the PD function, and different colors corresponds to different level-3 scores. For example, the first blue bar in the first block corresponds to  $\frac{I_{military}(1;T_3) - I_{military}(1;\tilde{T}_3)}{I_{military}(1;\tilde{T}_3)}$ , where  $T_3$  and  $\tilde{T}_3$  are the learned and baseline policy.

military outcomes through the regional safety measure (Figure 9c). Overall, our analysis suggests that the HES over-emphasized the importance of the military model for all three types of outcomes.

### 6.3 Learning the entire scoring system

Next, we consider learning both the two-way and three-way tables through all three levels of aggregation. In other words, we consider a policy class with the same aggregation structure as in the original HES, but potentially modifies the two-way and three-way tables used in the aggregation. Formally, we consider the following policy class,

$$\Pi_3 = \{\delta(\cdot; T_2, T_3) : T_2, T_3 \text{ is monotonic}\} \quad (15)$$

We use the same posterior CATE draws obtained in the previous analysis.

Unlike Section 6.2, this complex policy class makes it difficult to directly optimize the objective. Thus, in Appendix S5, we develop an optimization method based on directed acyclic graph (DAG) partitioning to solve this specific problem. As in the previous analysis, we compute the PD importance measure for each sub-model score.

Figure 10 presents the relative importance of the sub-model scores under the baseline policy and the optimal policy with a safety level  $\epsilon = 0.1$ . Each plot shows the scaled PD importance of the 19



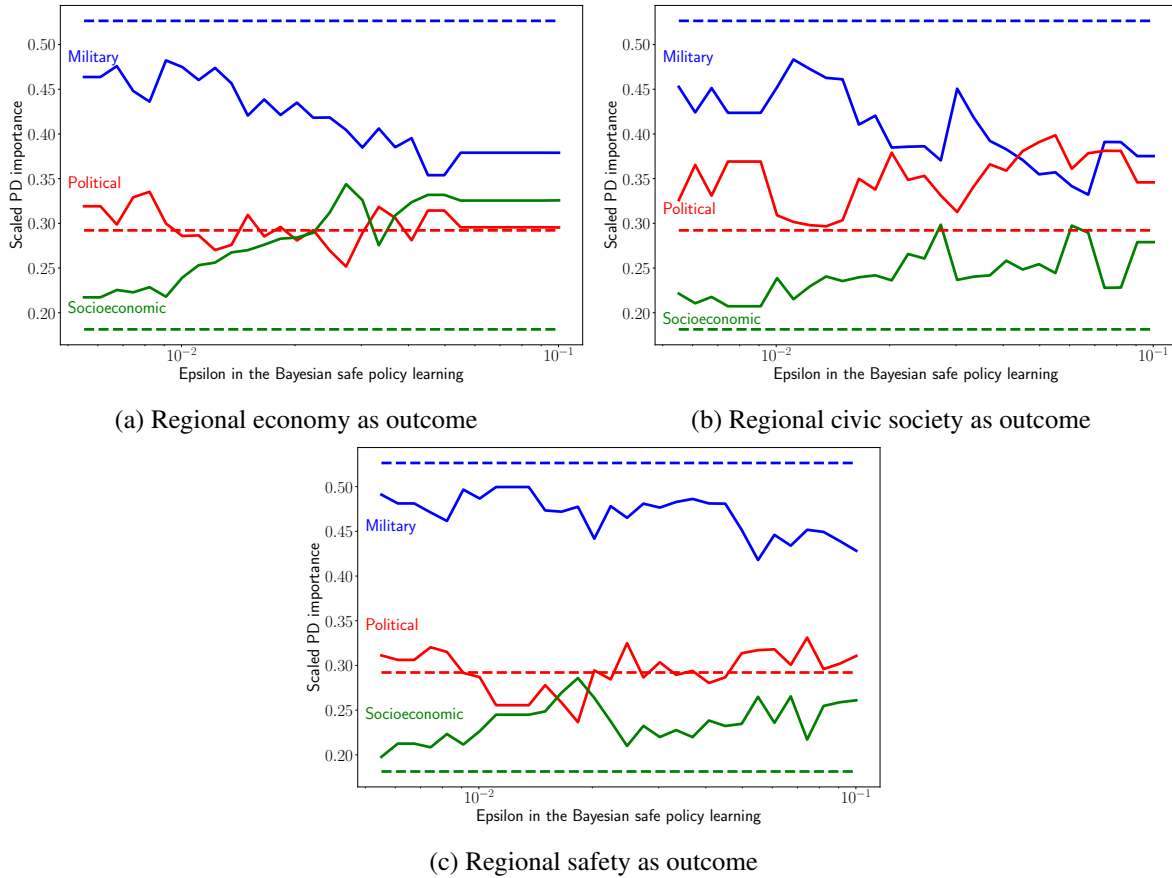
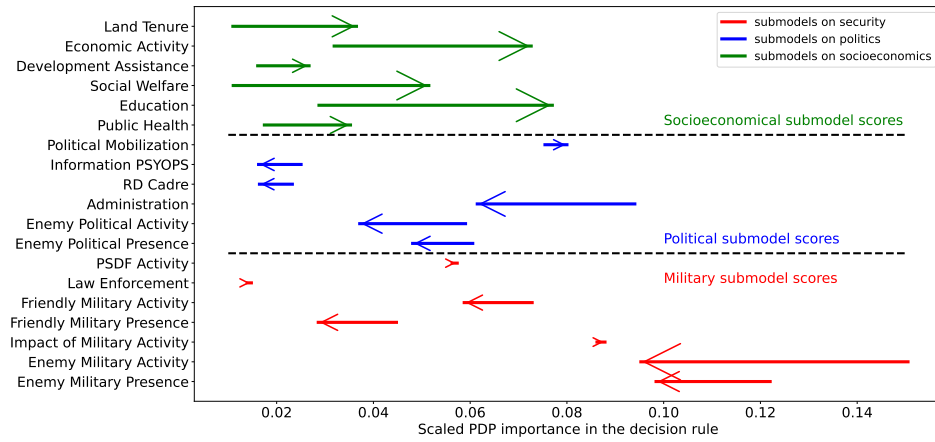


Figure 9: The scaled Partial Dependence (PD) importance of level-3 scores of the learned policy, as a function of the  $\epsilon$ . The solid line corresponds to the learned policy, and the dashed line indicates the baseline policy. Lines with different colors shows the PD importance of different level-3 scores.

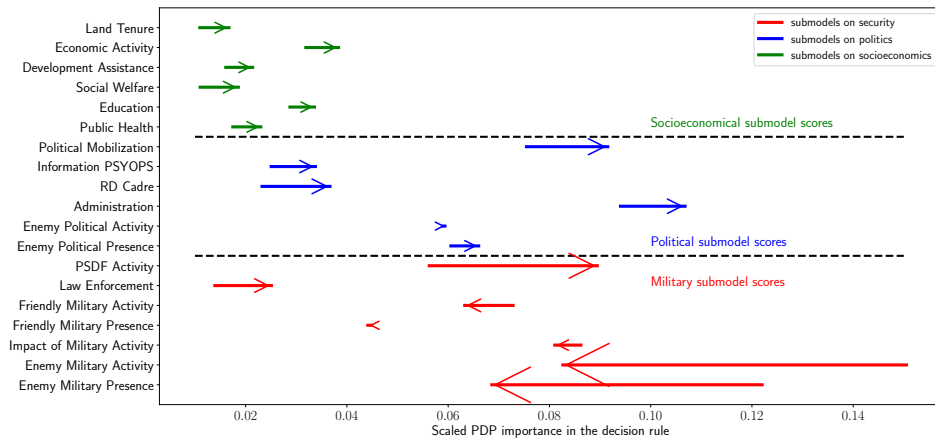
different sub-model scores under the baseline and learned policies for the three different outcomes: regional safety, economy, and civic society. Each arrow shows how the scaled PD importance changes from the baseline policy to the learned policy.

We find that when the outcome is either regional economy or civic society (Figures 10a and 10b), the learned policy puts less weight on the security sub-model scores than the baseline policy, with particularly large declines in the relative importance of enemy military activity and presence. Note, however, this is partially offset by an increase in the relative importance of PSDF (People’s Self-Defense Force) activity and law enforcement.

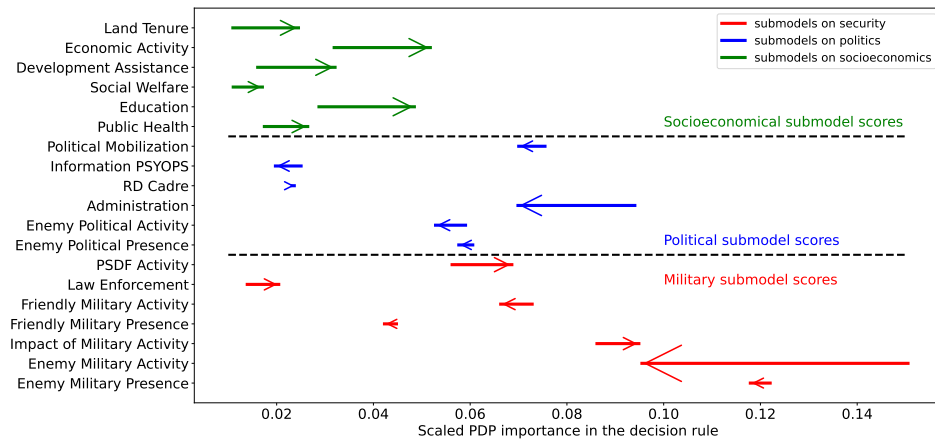
In contrast, the socioeconomic sub-model scores are more important when targeting all three outcomes, particularly so when targeting the economic outcome. Finally, the change in the relative importance of the political sub-model scores is more mixed; their importance only changes slightly when targeting regional safety (Figure 10c), generally declines when targeting the regional economy, and increases when targeting regional civic society.



(a) Regional economy as outcome



(b) Regional civic society as outcome



(c) Regional safety as outcome

Figure 10: The scaled PD importance of 19 different sub-model scores in the learned policy ( $\epsilon = 0.1$ ) and baseline policy with different outcomes. Each arrow indicates the change of the scaled PDP importance from the baseline policy to the learned policy.

## 7 Concluding Remarks

In this paper, we propose a new notion of average conditional risk, which represents the population proportion of groups that are worse off under a new, learned policy than the baseline policy. We then develop a Bayesian safe policy learning framework that limits this risk. The proposed methodology separates the estimation of heterogeneous treatment effects and policy optimization. This enables the use of flexible Bayesian nonparametric models while considering a complex policy class.

We apply the proposed methodology to the military security assessment during the Vietnam War. Substantively, our analysis shows that the HES—which was actually used during the war—attached too much importance to the security scores. In contrast, the Bayesian safe policy assigns greater weight to socioeconomic factors. Methodologically, we develop a stochastic optimization algorithm that is generally applicable to optimization over monotonic decision tables. Given the popularity of such decision rules in public policy and other settings, we believe that our optimization algorithm is of independent interest.

There are several directions for further research. First, while we take a Bayesian approach, it is of interest to consider a frequentist approach to controlling the average conditional risk (ACRisk) in policy learning. Second, our simulation study suggests that the posterior ACRisk constraint plays a role of regularization in policy optimization and an appropriate level of risk constraint can improve the average value of the learned policy. Better understanding how regularization improves policy learning is an important next step. Third, it is of interest to extend the proposed Bayesian policy learning framework to other types of constraints such as fairness and budget constraints.

# Supplementary Appendix

## S1 Three-way decision tables used in the HES

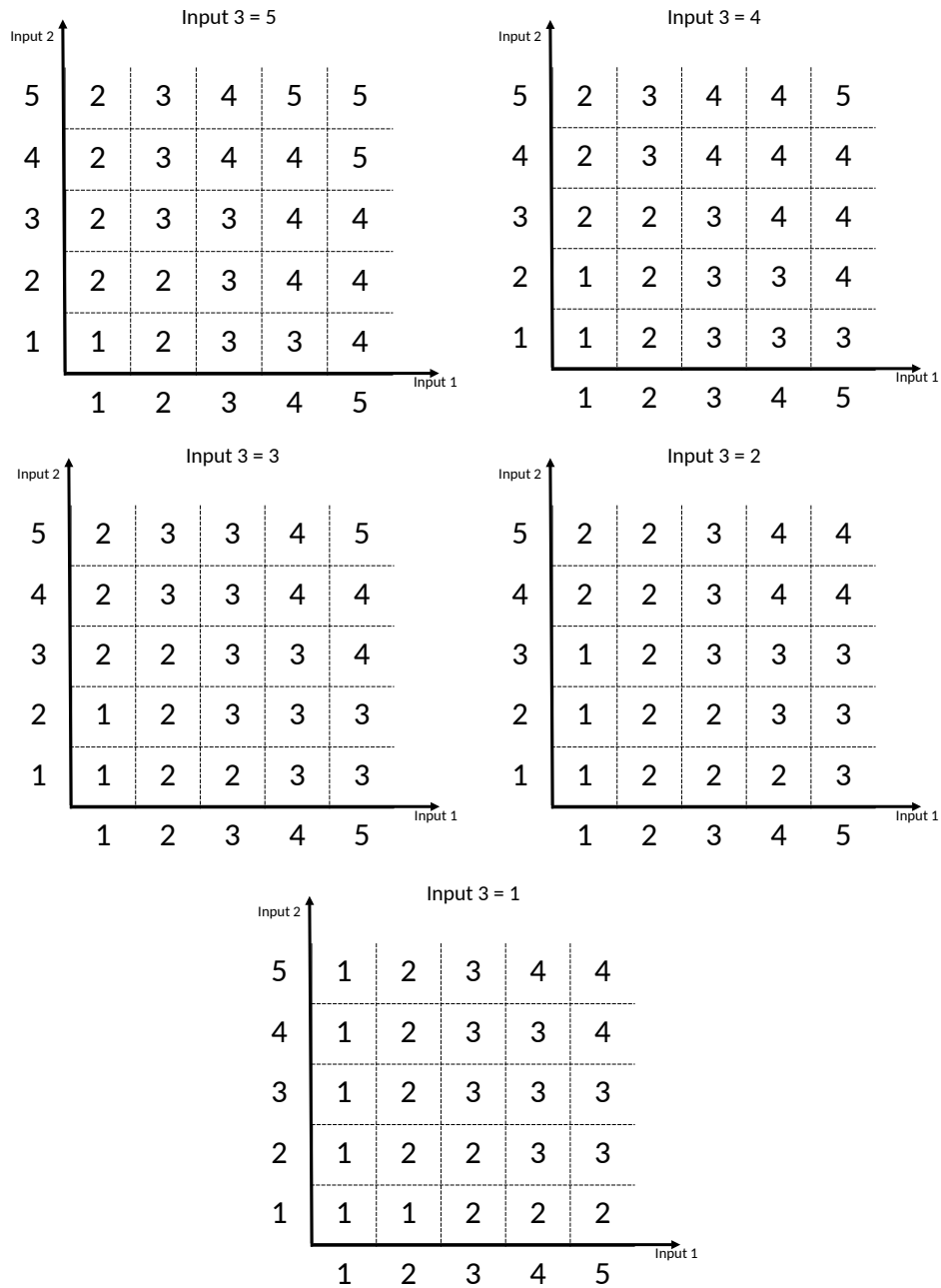


Figure S1: Three-way decision tables used in the HES. Each figure fixes the third input score and shows the output score for different combination of the first two inputs.

## S2 An additional figure and table

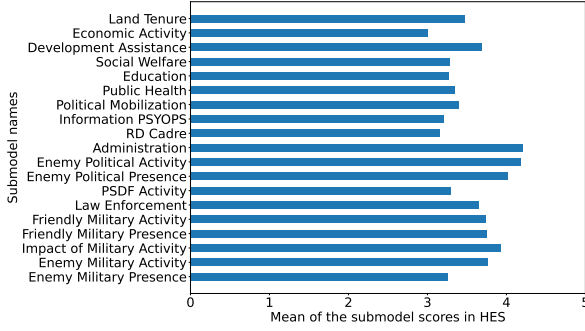


Figure S2: The mean of each sub-model score across the 1954 regions

Variable	Value
Number of regions	1954
Number of regions being attacked	1024
Average security score	3.34
Average regional safety outcome	0.53
Average regional economy outcome	0.51
Average civic society outcome	0.43

Table S1: Summary statistics on key measures

## S3 Proof of Theorem 1

We wish to show that the original chance-constraint optimization problem (see Equation (4))

$$\delta_{\text{safe}} = \underset{\delta \in \Pi}{\operatorname{argmax}} \mathbb{E} [V(\delta; \Theta) | \{Z_i\}_{i=1}^n], \quad (\text{S1})$$

$$\text{subject to } \mathbb{E} [R(\delta, \tilde{\delta}; \Theta) | \{Z_i\}_{i=1}^n] \leq \epsilon, \quad (\text{S2})$$

can be equivalently written as,

$$\delta_{\text{safe}} = \underset{\delta \in \Pi}{\operatorname{argmax}} \sum_{k=0}^{K-1} \int I(\delta(\mathbf{x}) = k) b_k(\mathbf{x}) dF(\mathbf{x}) \quad (\text{S3})$$

$$\text{subject to } \sum_{k=0}^{K-1} \int I(\delta(\mathbf{x}) = k) r_k(\mathbf{x}) dF(\mathbf{x}) \leq \epsilon, \quad (\text{S4})$$

where  $F(\mathbf{x})$  be the CDF of the covariate  $\mathbf{X}$ , and

$$\tau_k(\mathbf{x}, \theta) := \mathbb{E} [u(k, Y(k)) - u(\tilde{\delta}(\mathbf{x}), Y(\tilde{\delta}(\mathbf{x}))) | \mathbf{X} = \mathbf{x}, \Theta = \theta],$$

$$b_k(\mathbf{x}) := \mathbb{E} [\tau_k(\mathbf{x}, \Theta) | \{Z_i\}_{i=1}^n],$$

$$r_k(\mathbf{x}) := \mathbb{P} (\tau_k(\mathbf{x}, \Theta) < 0 | \{Z_i\}_{i=1}^n).$$

We first show the constraint given in Equation (S2) are equivalent to Equation (S4). By the definition of the posterior average conditional risk, we have

$$\begin{aligned} R(\delta, \tilde{\delta}; \Theta) &= \mathbb{P} \left( \mathbb{E} [u(\delta(\mathbf{X}), Y(\delta(\mathbf{X}))) | \mathbf{X}, \Theta] < \mathbb{E} [u(\tilde{\delta}(\mathbf{X}), Y(\tilde{\delta}(\mathbf{X}))) | \mathbf{X}, \Theta] \mid \Theta \right) \\ &= \mathbb{P} \left( \mathbb{E} [u(\delta(\mathbf{X}), Y(\delta(\mathbf{X}))) - u(\tilde{\delta}(\mathbf{X}), Y(\tilde{\delta}(\mathbf{X}))) | \mathbf{X}, \Theta] < 0 \mid \Theta \right) \end{aligned}$$

$$= \mathbb{P} \left( \sum_{k=0}^{K-1} \tau_k(\mathbf{X}, \Theta) I(\delta(\mathbf{X}) = k) < 0 \mid \Theta \right) \quad (\text{S5})$$

Therefore, Equation (S2) can be written as

$$\begin{aligned} \mathbb{E} \left[ R(\delta, \tilde{\delta}; \Theta) \mid \{Z_i\}_{i=1}^n \right] &= \mathbb{E} \left[ \mathbb{P} \left( \sum_{k=0}^{K-1} \tau_k(\mathbf{X}, \Theta) I(\delta(\mathbf{X}) = k) < 0 \mid \Theta \right) \mid \{Z_i\}_{i=1}^n \right] \\ &= \mathbb{E} \left[ \mathbb{E} \left[ I \left\{ \sum_{k=0}^{K-1} \tau_k(\mathbf{X}, \Theta) I(\delta(\mathbf{X}) = k) < 0 \right\} \mid \Theta \right] \mid \{Z_i\}_{i=1}^n \right]. \end{aligned}$$

Notice the inner probability is taken over the distribution of  $X$ , while the outer expectation is taken over the posterior distribution of  $\Theta$ . By the law of iterated expectation, We can write the above expression as,

$$\mathbb{E} \left[ \mathbb{E} \left[ I \left\{ \sum_{k=0}^{K-1} \tau_k(\mathbf{X}, \Theta) I(\delta(\mathbf{X}) = k) < 0 \right\} \mid \Theta \right] \mid \{Z_i\}_{i=1}^n \right] \quad (\text{S6})$$

$$= \mathbb{E} \left[ I \left\{ \sum_{k=0}^{K-1} \tau_k(\mathbf{X}, \Theta) I(\delta(\mathbf{X}) = k) < 0 \right\} \mid \{Z_i\}_{i=1}^n \right] \quad (\text{S7})$$

$$= \mathbb{E} \left[ \mathbb{E} \left[ I \left\{ \sum_{k=0}^{K-1} \tau_k(\mathbf{X}, \Theta) I(\delta(\mathbf{X}) = k) < 0 \right\} \mid \{Z_i\}_{i=1}^n, \mathbf{X} \right] \mid \{Z_i\}_{i=1}^n \right] \quad (\text{S8})$$

$$= \mathbb{E} \left[ \sum_{k=0}^{K-1} I(\delta(\mathbf{X}) = k) r_k(\mathbf{X}) \mid \{Z_i\}_{i=1}^n \right] \quad (\text{S9})$$

$$= \sum_{k=0}^{K-1} \int I(\delta(\mathbf{x}) = k) r_k(\mathbf{x}) dF(\mathbf{x}).$$

In Equation (S6), the inner expectation is taken over the distribution of the covariate  $\mathbf{X}$  and the outer expectation is taken over the posterior distribution of  $\Theta$ ; In Equation (S7), the expectation is taken over the distribution of  $\mathbf{X}$  and  $\Theta$ ; In Equation (S8), the inner expectation is taken over the posterior distribution of  $\Theta$  and the outer expectation is taken over the distribution of  $\mathbf{X}$ .

Similarly, for the optimization target, we have

$$\begin{aligned} &\mathbb{E} [V(\delta; \Theta) \mid \{Z_i\}_{i=1}^n] \\ &= \mathbb{E} [u(\delta(\mathbf{X}), Y(\delta(\mathbf{X}))) \mid \{Z_i\}_{i=1}^n] \quad (\text{S10}) \\ &= \mathbb{E} \left[ \mathbb{E} \left\{ u(\delta(\mathbf{X}), Y(\delta(\mathbf{X}))) \mid \{Z_i\}_{i=1}^n, \mathbf{X} \right\} \mid \{Z_i\}_{i=1}^n \right] \\ &= \mathbb{E} \left[ \mathbb{E} \left\{ \sum_{k=0}^{K-1} u(\delta(\mathbf{X}), Y(k)) I(\delta(\mathbf{X}) = k) \mid \{Z_i\}_{i=1}^n, \mathbf{X} \right\} \mid \{Z_i\}_{i=1}^n \right] \\ &= \mathbb{E} \left[ \mathbb{E} \left\{ \sum_{k=0}^{K-1} \tau_k(\mathbf{X}, \Theta) I(\delta(\mathbf{X}) = k) \mid \{Z_i\}_{i=1}^n, \mathbf{X} \right\} \mid \{Z_i\}_{i=1}^n \right] + \text{const.} \end{aligned}$$

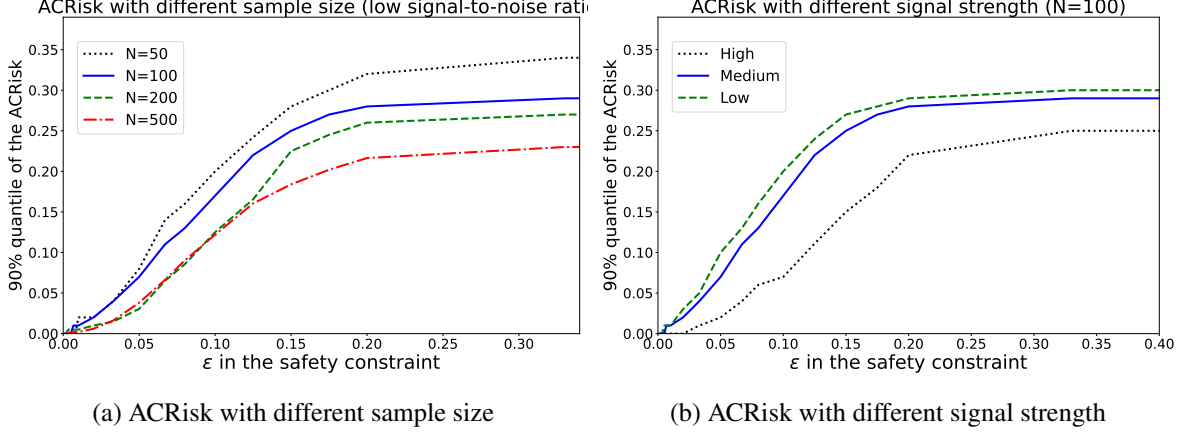


Figure S3: 90 % quantile of the ACRisk for learned policy among 2000 simulations. The CATE is estimated with BCF and covariates have overlap

$$\begin{aligned}
&= \mathbb{E} \left[ \sum_{k=0}^{K-1} I(\delta(\mathbf{X}) = k) b_k(\mathbf{X}) \middle| \{Z_i\}_{i=1}^n \right] + \text{const.} \\
&= \sum_{k=0}^{K-1} \int I(\delta(\mathbf{x}) = k) b_k(\mathbf{x}) dF(\mathbf{x}) + \text{const.}
\end{aligned} \tag{S11}$$

where const. represents the term that is not a function of  $\delta$ . In Equation (S10), the expectation is taken over the distribution of  $X$ , the posterior distribution of  $\Theta$ , and the conditional distribution of  $Y$  given  $X, \Theta$ . Then, we first compute the expectation over  $\Theta$  and the conditional distribution of  $Y$  given  $X$ . Taking the expectation over the distribution of  $X$  gives Equation (S11). Thus,

$$\operatorname{argmax}_{\delta \in \Pi} \mathbb{E} [V(\delta; \Theta) | \{Z_i\}_{i=1}^n] \iff \operatorname{argmax}_{\delta \in \Pi} \sum_{k=0}^{K-1} \int I(\delta(\mathbf{x}) = k) b_k(\mathbf{x}) dF(\mathbf{x}).$$

□

## S4 Additional Simulation Results

Here we present additional detailed simulation results.

### S4.1 The tail distribution of the empirical ACRisk

In Section 5, we discuss the average ACRisk of the learned policy in multiple simulations. However, sometimes we may be also interested in the tail distribution for the ACRisk of learned policy. Therefore, we present the 90% quantile of the ACRisk for learned policy among 2000 simulations. Figure S3 and S4 shows how the 90% quantile of the ACRisk changes with different sample size, signal strength, smoothness for prior of the CATE, and the strength of the prior. The results are essentially similar to the average ACRisk of learned policies,



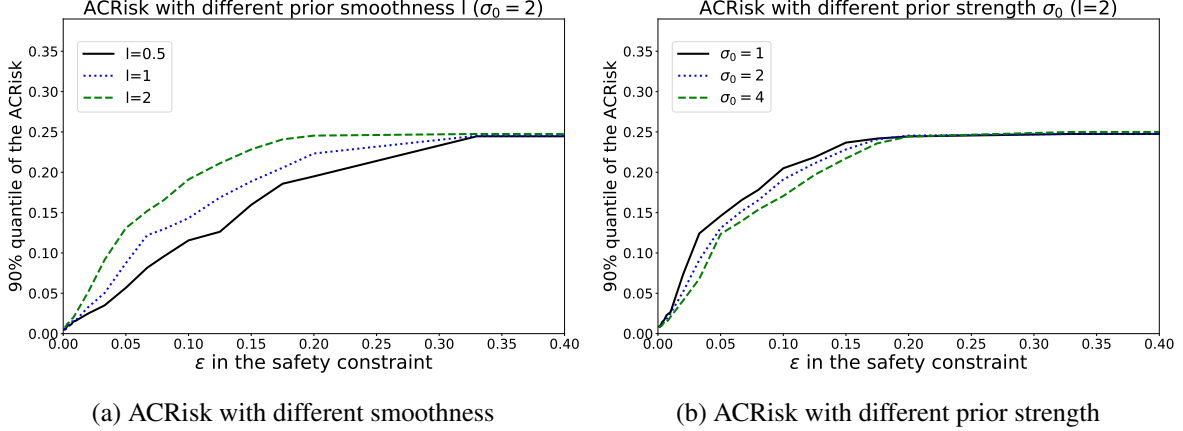


Figure S4: 90 % quantile of the ACRisk for learned policy among 2000 simulations. The CATE is estimated with a GP and there is no covariate overlap.

## S4.2 Simulation results with Binary outcomes

The previous simulation design focused on continuous outcomes. Our method also applies to binary outcome data, and here we present simulation results when the outcome is binary. Generally speaking, we see a similar pattern as the case of continuous outcomes in various settings.

We use a similar setup as in Section 5 where the covariates  $\mathbf{X} = (X_1, X_2)$  and  $X_1, X_2 \stackrel{\text{i.i.d}}{\sim} \text{Uniform}[-1, 1]$ . We use the same Scenario I (with covariate overlap) and Scenario II (without covariate overlap) for generating the decision  $D$  in the data. For the outcome, we let

$$Y | \mathbf{X} \sim \text{Bernoulli} \left( \text{expit} \left( \frac{X_1}{2} + \frac{X_2}{2} + \gamma \{3I(X_1 > 0, X_2 > 0) - \frac{3}{2}\} D | X_1 || X_2 | \right) \right),$$

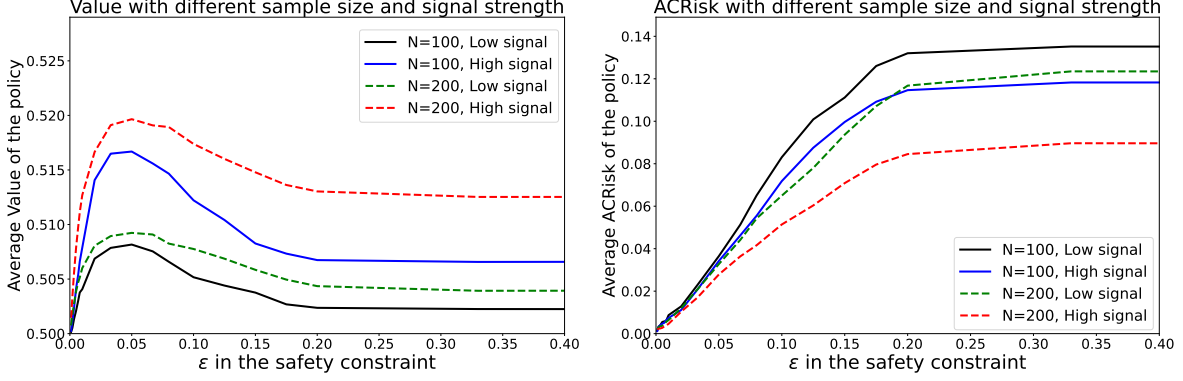
where we consider a strong signal case  $\gamma = 2$  and a weak signal case  $\gamma = 1$ . We vary the number of observations  $n \in \{50, 100, 200\}$ , and we use a Gaussian Process (GP) to model the CATE.

**With covariate overlap** In the case with covariate overlap, there is no need for extrapolation. Therefore, we use a weak prior for the GP and specify the mean function  $m(x) = 0$ , the kernel function as a Matern kernel with  $\sigma_0 = 4, l = 0.5$ . We show how the average ACRisk and the value changes as a function of the safety constraint  $\epsilon$  under different sample size and signal strength in Figure S5.

**Without covariate overlap** When there is no covariate overlap, the CATE must be extrapolated. We fix the sample size to 200 and the signal strength  $\gamma = 2$  and investigate the average Value and ACRisk for learned policies with different priors. Figure S6 and Figure S7 shows the average Value and ACRisk of the learned policy as a function of the safety constraint  $\epsilon$  under different prior smoothness and prior strength.

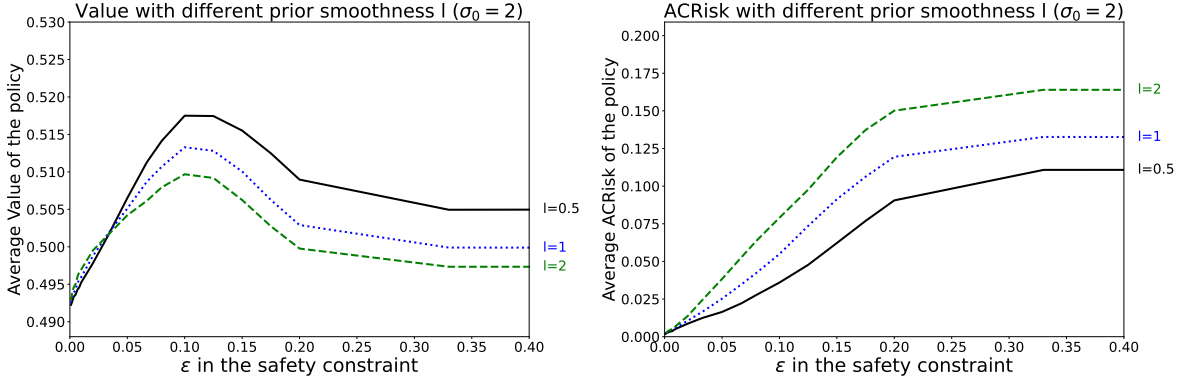
## S5 Optimization for Monotonic Decision Tables

In this section, we develop an optimization algorithm applicable to monotonic decision tables where the output of a decision table is non-decreasing in each input dimension.



(a) Average Value with different sample size and signal strength (b) Average ACRisk with different sample size and signal strength

Figure S5: Average Value and ACRisk for the learned policy among 2000 simulations. The CATE is estimated with GP and covariates have overlap



(a) Average Value

(b) Average ACRisk

Figure S6: Average Value and ACRisk for learned policies using data without covariate overlap, varying the safety constraint and prior smoothness for the CATE.

### S5.1 Problem definition

We define the *monotonic decision table* as below:

**Definition S1** (Monotonic decision tables). Suppose  $\mathcal{X}_1, \mathcal{X}_2, \dots, \mathcal{X}_p, \mathcal{Y}$  are finite totally ordered sets,  $T$  is a function that maps  $x \in \mathcal{X} = \mathcal{X}_1 \times \mathcal{X}_2 \times \dots \times \mathcal{X}_p$  to  $\mathcal{Y}$ . Then,  $T$  is a monotonic decision table if and only if the following condition holds,

$$\forall x = \{x_i\}_{i=1}^p, x' = \{x'_i\}_{i=1}^p \in \mathcal{X} \text{ where } x_i \leq x'_i \text{ for } 1 \leq i \leq p, T(x_1, \dots, x_p) \leq T(x'_1, \dots, x'_p)$$

We consider the following general optimization problem over monotonic decision tables.

**Definition S2** (Optimization with monotonic decision tables). Suppose  $f, g$  are functions that map a monotonic decision table  $T$  into a real-valued output. We consider the problem of finding an optimal

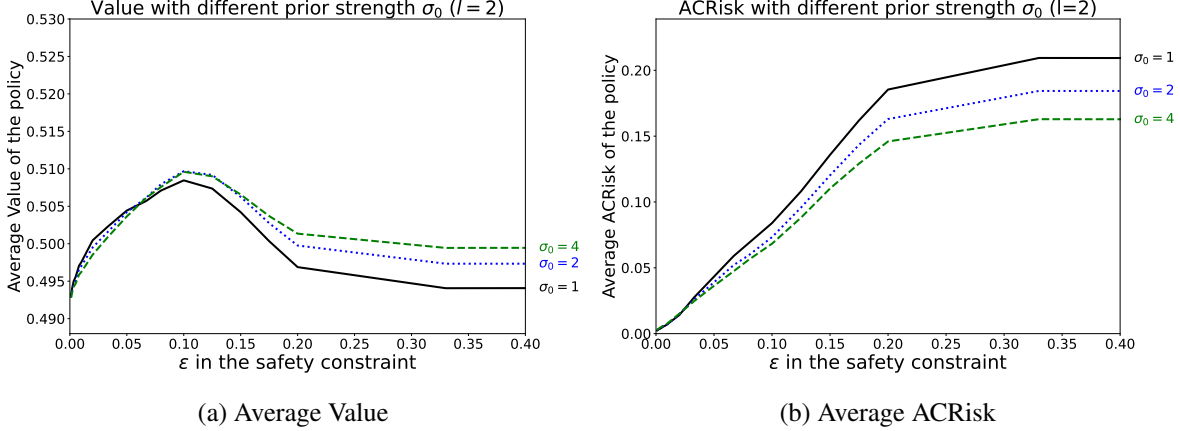


Figure S7: Average Value and ACRisk for learned policies using data without covariate overlap, varying the safety constraint and prior strength for the CATE.

monotonic decision table  $T_{opt}$  as defined below:

$$T_{opt} := \underset{T}{\operatorname{argmin}} f(T) \text{ subject to } g(T) \geq 0 \quad (\text{S12})$$

In general, optimization over monotonic decision tables with the form given in Equation (S12) is difficult to solve. Although one could enumerate all possible monotonic decision tables and their corresponding  $f(T)$ ,  $g(T)$ , the number of enumerations is equal to  $\mathcal{Y}^{|\mathcal{X}|} = \mathcal{Y}^{|\mathcal{X}_1| \times |\mathcal{X}_2| \times \dots \times |\mathcal{X}_p|}$ , which grows exponentially as the size of the decision table increases. In our application, we wish to simultaneously learn one two-way decision table and one three-way decision table, yielding a total of  $5^{25} \times 5^{125} = 5^{150}$  enumerations. We would like to avoid enumerating these many possibilities.

Therefore, we use a Markov chain Monte Carlo (MCMC)-based stochastic algorithm for optimizing over monotonic decision tables by adopting ideas from the graph theory. Specifically, we represent a monotonic decision tables as an equivalent directed acyclic graph (DAG) where the directed edges indicates the monotonicity conditions, and optimize over monotonic decision tables by sampling the DAGs using an MCMC algorithm.

## S5.2 Graph representation for monotonic decision tables

Monotonic decision tables can be equivalently represented as directed acyclic graphs (DAGs). We represent different inputs of decision tables as vertices of the DAG, and the monotonicity constraint on the decision table as directed edges in the graph. For example, Figure S8 shows the graph representation for the original two-way decision tables in the HES (Figure 2). The two-way decision table has  $5 \times 5 = 25$  different inputs, which corresponds to the 25 vertices in the graph. The edges in the DAG indicate the monotonicity constraint that the output should satisfy according to the decision table. For example, in Figure S8, there is a directed edge from vertex  $[1, 1]$  to vertex  $[1, 2]$ , which means that the output of the decision table for input  $[1, 1]$  should be no greater than the output for input  $[1, 2]$ .

With this representation, finding a decision table from  $\mathcal{X}$  to  $\mathcal{Y}$  is equivalent to finding a graph par-

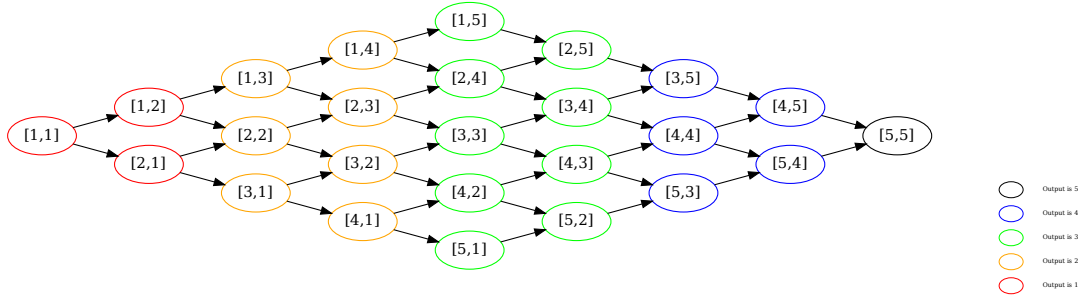


Figure S8: The DAG representation of the original 2-way decision table in the HES. Each vertex corresponds to an input of the 2-way table, and directed edges indicate the relative order the corresponding output should satisfy based on the monotonicity constraint. The color of the nodes indicate the output of the 2-way decision table in the original HES.

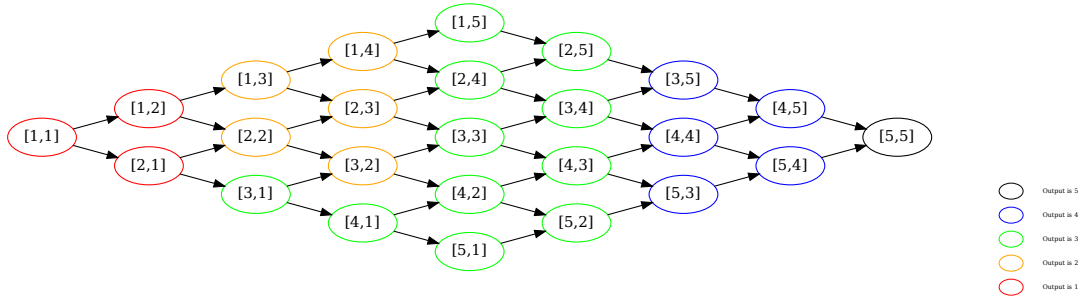


Figure S9: An example of partition for a decision table that does not satisfy the monotonicity constraint. There is a directed edge from  $[3, 1]$  to  $[3, 2]$ , but the output for  $[3, 1]$  is larger than the output for  $[3, 2]$ .

tition that separate the DAG into  $|\mathcal{Y}|$  areas where vertices in the same area have the same output scores. A monotonicity constraint on the decision table is equivalently translated to an *acyclic* constraint on the partition, where we forbid any directed edges from a node with larger output to a node with a smaller outcome (Herrmann et al., 2017, 2019).

Figure S8 shows the graph partition corresponding to the original two-way decision table in the HES, where the color of a node indicates the partition. This satisfies the monotonicity constraint. In contrast, Figure S9 shows a different partition that does not satisfy the monotonicity constraint. There is a directed edge from  $[3, 1]$  to  $[3, 2]$ , but the output for  $[3, 1]$  is larger than the output for  $[3, 2]$ .

### S5.3 Optimization by sampling partitions of the DAGs

We optimize over monotonic decision tables by finding optimal acyclic partitions of the corresponding DAGs. We propose an MCMC-based stochastic algorithm for sampling acyclic partitions of the DAGs and optimize over it.

To do this, we first sample a *topological sort* of a DAG (Karzanov and Khachiyan, 1990) and then segment the topological sort into  $|\mathcal{Y}|$  pieces to obtain a partition of the DAG.

---

**Algorithm 2:** Stochastic Optimization Algorithm for Monotonic Decision Tables

---

**Data:** A DAG  $\mathcal{G}$  that contains all the potential inputs of the decision table and relations from monotonicity constraints; a Markov chain  $\mathcal{M}$  that generates an acyclic partial partition of  $\mathcal{G}$  with a uniform stationary distribution; An initial monotonic decision table  $T_0$  and corresponding state  $S_0$  of  $\mathcal{M}$ .

```
1 for  $0 \leq r \leq R$  do
2    $S_{r0} \leftarrow S_r$ 
3    $T_{r0} \leftarrow T_r$ 
4   for  $1 \leq k \leq K$  do
5      $S_{rk} \leftarrow \mathcal{M}(S_{r(k-1)})$ 
6      $T_{rk} \leftarrow$  Decision table that corresponds to  $S_{rk}$ 
7   end for
8    $S_{r+1} \leftarrow \arg \min_{T \in \{T_{r0}, T_{r1}, \dots, T_{rK}\}} f(T)$  subject to  $g(T) \geq 0$ 
9    $T_{r+1} \leftarrow$  Decision table corresponds to  $S_{r+1}$ ;
10 end for
11 Return  $T_{R+1}$ 
```

---

**Definition S3.** (Topological sorts on DAGs) A topological sort of a directed acyclic graph is a linear ordering of its vertices such that for every directed edge  $uv$  from vertex  $u$  to vertex  $v$ ,  $u$  comes before  $v$  in the ordering.

We take advantage of the fact that any segmentation of a topological sort corresponds to an acyclic partition and produces a decision table satisfying the monotonicity constraint. Conversely, for any decision table satisfying the monotonicity constraint, there will be a corresponding topological sort and segmentation that produces the decision table. We use the MCMC algorithm of [Karzanov and Khachiyan \(1990\)](#) to sample a topological sort from the DAG and a random walk to sample segmentations of the topological sorts. This gives us a Markov chain that generates random acyclic partitions. Finally, we use a *short-burst* algorithm to use the MCMC sampling algorithm for optimization ([Cannon et al., 2023](#)). Algorithm 2 formally describes our optimization procedure.

## References

- Athey, S. and Wager, S. (2021). Policy learning with observational data. *Econometrica*, 89(1):133–161.
- Bai, C., Wang, L., Yang, Z., Deng, Z., Garg, A., Liu, P., and Wang, Z. (2022). Pessimistic bootstrapping for uncertainty-driven offline reinforcement learning. *arXiv preprint arXiv:2202.11566*.
- Ben-Michael, E., Greiner, D. J., Imai, K., and Jiang, Z. (2021). Safe policy learning through extrapolation: Application to pre-trial risk assessment. *arXiv preprint arXiv:2109.11679*.
- Ben-Michael, E., Imai, K., and Jiang, Z. (2022). Policy learning with asymmetric utilities. *arXiv preprint arXiv:2206.10479*.
- Beygelzimer, A. and Langford, J. (2009). The offset tree for learning with partial labels. In *Proceedings of the 15th ACM SIGKDD international conference on Knowledge discovery and data mining*, pages 129–138.
- Branson, Z., Rischard, M., Bornn, L., and Miratrix, L. W. (2019). A nonparametric bayesian methodology for regression discontinuity designs. *Journal of Statistical Planning and Inference*, 202:14–30.
- Buckman, J., Gelada, C., and Bellemare, M. G. (2020). The importance of pessimism in fixed-dataset policy optimization. *arXiv preprint arXiv:2009.06799*.
- Cannon, S., Goldbloom-Helzner, A., Gupta, V., Matthews, J., and Suwal, B. (2023). Voting rights, markov chains, and optimization by short bursts. *Methodology and Computing in Applied Probability*, 25(1):36.
- Carpenter, B., Gelman, A., Hoffman, M. D., Lee, D., Goodrich, B., Betancourt, M., Brubaker, M., Guo, J., Li, P., and Riddell, A. (2017). Stan: A probabilistic programming language. *Journal of statistical software*, 76(1).
- Chen, J. and Jiang, N. (2022). Offline reinforcement learning under value and density-ratio realizability: the power of gaps. *arXiv preprint arXiv:2203.13935*.
- Chipman, H. A., George, E. I., and McCulloch, R. E. (2010). Bart: Bayesian additive regression trees.
- Daddis, G. A. (2012). The problem of metrics: Assessing progress and effectiveness in the Vietnam War. *War in History*, 19(1):73–98.
- Delage, E. and Mannor, S. (2007). Percentile optimization in uncertain markov decision processes with application to efficient exploration. In *Proceedings of the 24th international conference on Machine learning*, pages 225–232.
- Delage, E. and Mannor, S. (2010). Percentile optimization for markov decision processes with parameter uncertainty. *Operations research*, 58(1):203–213.

- Dell, M. and Querubin, P. (2018). Nation building through foreign intervention: Evidence from discontinuities in military strategies. *The Quarterly Journal of Economics*, 133(2):701–764.
- Ding, P. and Li, F. (2018). Causal inference: a missing data perspective. *Statistical Science*, 33(2):214–237.
- Dudík, M., Langford, J., and Li, L. (2011). Doubly robust policy evaluation and learning. *Proceedings of the 28th International Conference on Machine Learning*.
- Farina, M., Giulioni, L., and Scattolini, R. (2016). Stochastic linear model predictive control with chance constraints – a review. *Journal of Process Control*, 44:53–67.
- Filar, J. A., Krass, D., and Ross, K. W. (1995). Percentile performance criteria for limiting average markov decision processes. *IEEE Transactions on Automatic Control*, 40(1):2–10.
- Friedman, J. H. (2001). Greedy function approximation: a gradient boosting machine. *Annals of statistics*, pages 1189–1232.
- Garcia, J. and Fernández, F. (2015). A comprehensive survey on safe reinforcement learning. *Journal of Machine Learning Research*, 16(1):1437–1480.
- Geibel, P. and Wysotzki, F. (2005). Risk-sensitive reinforcement learning applied to control under constraints. *Journal of Artificial Intelligence Research*, 24:81–108.
- Greenwell, B. M., Boehmke, B. C., and McCarthy, A. J. (2018). A simple and effective model-based variable importance measure. *arXiv preprint arXiv:1805.04755*.
- Greiner, J., Halen, R., Stubenberg, M., and Griffin, C. L. (2020). Randomized control trial evaluation of the implementation of the psa-dmf system in dane county, wi.
- Hahn, P. R., Murray, J. S., and Carvalho, C. M. (2020). Bayesian regression tree models for causal inference: Regularization, confounding, and heterogeneous effects (with discussion). *Bayesian Analysis*, 15(3):965–1056.
- Herrmann, J., Kho, J., Uçar, B., Kaya, K., and Çatalyürek, Ü. V. (2017). Acyclic partitioning of large directed acyclic graphs. In *2017 17th IEEE/ACM international symposium on cluster, cloud and grid computing (CCGRID)*, pages 371–380. IEEE.
- Herrmann, J., Özkaya, M. Y., Uçar, B., Kaya, K., and Çatalyürek, U. V. (2019). Multilevel algorithms for acyclic partitioning of directed acyclic graphs. *SIAM Journal on Scientific Computing*, 41(4):A2117–A2145.
- Hill, J. L. (2011). Bayesian nonparametric modeling for causal inference. *Journal of Computational and Graphical Statistics*, 20(1):217–240.

- Imai, K., Jiang, Z., Greiner, D. J., Halen, R., and Shin, S. (2023). Experimental evaluation of computer-assisted human decision-making: Application to pretrial risk assessment instrument (with discussion). *Journal of the Royal Statistical Society, Series A (Statistics in Society)*, 186(2):167–189.
- Jin, Y., Ren, Z., Yang, Z., and Wang, Z. (2022). Policy learning” without”overlap: Pessimism and generalized empirical bernstein’s inequality. *arXiv preprint arXiv:2212.09900*.
- Jin, Y., Yang, Z., and Wang, Z. (2021). Is pessimism provably efficient for offline rl? In *International Conference on Machine Learning*, pages 5084–5096. PMLR.
- Kallus, N. (2018). Balanced policy evaluation and learning. *Advances in neural information processing systems*, 31.
- Kallus, N. (2022). What’s the harm? sharp bounds on the fraction negatively affected by treatment. *arXiv preprint arXiv:2205.10327*.
- Kallus, N. and Zhou, A. (2021). Minimax-optimal policy learning under unobserved confounding. *Management Science*, 67(5):2870–2890.
- Kamath, P. S., Wiesner, R. H., Malinchoc, M., Kremers, W., Therneau, T. M., Kosberg, C. L., D’Amico, G., Dickson, E. R., and Kim, W. R. (2001). A model to predict survival in patients with end-stage liver disease. *Hepatology*, 33(2):464–470.
- Karzanov, A. and Khachiyan, L. (1990). *On the conductance of order Markov chains*. Rutgers University, Department of Computer Science, Laboratory for Computer . . . .
- Kitagawa, T. and Tetenov, A. (2018). Who should be treated? empirical welfare maximization methods for treatment choice. *Econometrica*, 86(2):591–616.
- Lauer, J. (2017). *Creditworthy: A History of Consumer Surveillance and Financial Identity in America*. Columbia University Press.
- Li, A., Jiang, S., Sun, Y., and Pearl, J. (2022a). Unit selection: Learning benefit function from finite population data. *arXiv preprint arXiv:2210.08203*.
- Li, F., Ding, P., and Mealli, F. (2022b). Bayesian causal inference: A critical review. *arXiv preprint arXiv:2206.15460*.
- Li, L., Chu, W., Langford, J., and Schapire, R. E. (2010). A contextual-bandit approach to personalized news article recommendation. In *Proceedings of the 19th international conference on World wide web*, pages 661–670.
- Luedtke, A. R. and Van Der Laan, M. J. (2016). Statistical inference for the mean outcome under a possibly non-unique optimal treatment strategy. *Annals of statistics*, 44(2):713.



- Mowbray, M., Petsagkourakis, P., del Rio-Chanona, E. A., and Zhang, D. (2022). Safe chance constrained reinforcement learning for batch process control. *Computers & chemical engineering*, 157:107630.
- Nahum-Shani, I., Smith, S. N., Spring, B. J., Collins, L. M., Witkiewitz, K., Tewari, A., and Murphy, S. A. (2018). Just-in-time adaptive interventions (jitais) in mobile health: key components and design principles for ongoing health behavior support. *Annals of Behavioral Medicine*, 52(6):446–462.
- Neyman, J. (1990 [1923]). On the application of probability theory to agricultural experiments. essay on principles. section 9. *Statistical Science*, 5(4):465–472.
- PACAF, H. Q. (1969). Tacc fragging procedures. *Project CHECO Southeast Asia Report*.
- Pu, H. and Zhang, B. (2020). Estimating optimal treatment rules with an instrumental variable: A partial identification learning approach. *arXiv preprint arXiv:2002.02579*.
- Qian, M. and Murphy, S. A. (2011). Performance guarantees for individualized treatment rules. *Annals of statistics*, 39(2):1180.
- Rashidinejad, P., Zhu, B., Ma, C., Jiao, J., and Russell, S. (2021). Bridging offline reinforcement learning and imitation learning: A tale of pessimism. *Advances in Neural Information Processing Systems*, 34:11702–11716.
- Rasmussen, C. E. and Williams, C. K. I. (2006). Gaussian processes for machine learning. The MIT Press.
- Rosenbaum, P. R. and Rubin, D. B. (1983). The central role of the propensity score in observational studies for causal effects. *Biometrika*, 70(1):41–55.
- Rubin, D. B. (1974). Estimating causal effects of treatments in randomized and nonrandomized studies. *Journal of educational Psychology*, 66(5):688.
- Rubin, D. B. (1980). Randomization analysis of experimental data: The fisher randomization test comment. *Journal of the American statistical association*, 75(371):591–593.
- Sato, M., Kimura, H., and Kobayashi, S. (2001). Td algorithm for the variance of return and mean-variance reinforcement learning. *Transactions of the Japanese Society for Artificial Intelligence*, 16(3):353–362.
- Schwarm, A. T. and Nikolaou, M. (1999). Chance-constrained model predictive control. *AIChE Journal*, 45(8):1743–1752.
- Schwartz, E. M., Bradlow, E. T., and Fader, P. S. (2017). Customer acquisition via display advertising using multi-armed bandit experiments. *Marketing Science*, 36(4):500–522.

- Shi, L., Li, G., Wei, Y., Chen, Y., and Chi, Y. (2022). Pessimistic q-learning for offline reinforcement learning: Towards optimal sample complexity. *arXiv preprint arXiv:2202.13890*.
- Swaminathan, A. and Joachims, T. (2015). Batch learning from logged bandit feedback through counterfactual risk minimization. *The Journal of Machine Learning Research*, 16(1):1731–1755.
- Taddy, M., Gardner, M., Chen, L., and Draper, D. (2016). A nonparametric bayesian analysis of heterogeneous treatment effects in digital experimentation. *Journal of Business & Economic Statistics*, 34(4):661–672.
- Tang, L., Rosales, R., Singh, A., and Agarwal, D. (2013). Automatic ad format selection via contextual bandits. In *Proceedings of the 22nd ACM international conference on Information & Knowledge Management*, pages 1587–1594.
- Uehara, M. and Sun, W. (2021). Pessimistic model-based offline reinforcement learning under partial coverage. *arXiv preprint arXiv:2107.06226*.
- Vakili, S. and Zhao, Q. (2015). Mean-variance and value at risk in multi-armed bandit problems. In *2015 53rd Annual Allerton Conference on Communication, Control, and Computing (Allerton)*, pages 1330–1335. IEEE.
- Vitus, M. P., Zhou, Z., and Tomlin, C. J. (2015). Stochastic control with uncertain parameters via chance constrained control. *IEEE Transactions on Automatic Control*, 61(10):2892–2905.
- Wei, D., Nair, R., Dhurandhar, A., Varshney, K. R., Daly, E. M., and Singh, M. (2022). On the safety of interpretable machine learning: A maximum deviation approach. *arXiv preprint arXiv:2211.01498*.
- Xie, T., Cheng, C.-A., Jiang, N., Mineiro, P., and Agarwal, A. (2021). Bellman-consistent pessimism for offline reinforcement learning. *Advances in neural information processing systems*, 34:6683–6694.
- Yan, Y., Li, G., Chen, Y., and Fan, J. (2022). The efficacy of pessimism in asynchronous q-learning. *arXiv preprint arXiv:2203.07368*.
- Yin, M. and Wang, Y.-X. (2021). Towards instance-optimal offline reinforcement learning with pessimism. *Advances in neural information processing systems*, 34:4065–4078.
- Zanette, A., Wainwright, M. J., and Brunskill, E. (2021). Provable benefits of actor-critic methods for offline reinforcement learning. *Advances in neural information processing systems*, 34:13626–13640.
- Zhang, B., Tsiatis, A. A., Davidian, M., Zhang, M., and Laber, E. (2012). Estimating optimal treatment regimes from a classification perspective. *Stat*, 1(1):103–114.
- Zhang, Y., Ben-Michael, E., and Imai, K. (2022). Safe policy learning under regression discontinuity designs. *arXiv preprint arXiv:2208.13323*.

- Zhao, Y., Zeng, D., Rush, A. J., and Kosorok, M. R. (2012). Estimating individualized treatment rules using outcome weighted learning. *Journal of the American Statistical Association*, 107(499):1106–1118.
- Zhou, X., Mayer-Hamblett, N., Khan, U., and Kosorok, M. R. (2017). Residual weighted learning for estimating individualized treatment rules. *Journal of the American Statistical Association*, 112(517):169–187.
- Zhou, Z., Athey, S., and Wager, S. (2022). Offline multi-action policy learning: Generalization and optimization. *Operations Research*.